

AD-A 152 195

AD A 152 695

AD-E401 305

TECHNICAL REPORT ARLCD-TR-84026

**DESIGN OF AMMUNITION GRIPPER FOR 155-MM ROBOTIC HOWITZER**

ROBERT M. NITZSCHE

TECHNICAL  
LIBRARY

MARCH 1985



**U.S. ARMY ARMAMENT RESEARCH AND DEVELOPMENT CENTER**

LARGE CALIBER WEAPON SYSTEMS LABORATORY

DOVER, NEW JERSEY

APPROVED FOR PUBLIC RELEASE; DISTRIBUTION UNLIMITED.

**The views, opinions, and/or findings contained in this report are those of the author(s) and should not be construed as an official Department of the Army position, policy, or decision, unless so designated by other documentation.**

**The citation in this report of the names of commercial firms or commercially available products or services does not constitute official endorsement by or approval of the U.S. Government.**

**Destroy this report when no longer needed. Do not return to the originator.**

## UNCLASSIFIED

SECURITY CLASSIFICATION OF THIS PAGE (When Data Entered)

REPORT DOCUMENTATION PAGE		READ INSTRUCTIONS BEFORE COMPLETING FORM												
1. REPORT NUMBER Technical Report ARLCD-TR-84026	2. GOVT ACCESSION NO.	3. RECIPIENT'S CATALOG NUMBER												
4. TITLE (and Subtitle) DESIGN OF AMMUNITION GRIPPER FOR 155-mm ROBOTIC HOWITZER		5. TYPE OF REPORT & PERIOD COVERED May - September 1983												
		6. PERFORMING ORG. REPORT NUMBER												
7. AUTHOR(s) Robert M. Nitzsche		8. CONTRACT OR GRANT NUMBER(s)												
9. PERFORMING ORGANIZATION NAME AND ADDRESS ARDC, LCWSL Weapons Div (SMCAR-LCW-E) Dover, NJ 07801-5001		10. PROGRAM ELEMENT, PROJECT, TASK AREA & WORK UNIT NUMBERS												
11. CONTROLLING OFFICE NAME AND ADDRESS ARDC, TSD STINFO Div (SMCAR-TSS) Dover, NJ 07801-5001		12. REPORT DATE March 1985												
		13. NUMBER OF PAGES 109												
14. MONITORING AGENCY NAME & ADDRESS (if different from Controlling Office)		15. SECURITY CLASS. (of this report) Unclassified												
		15a. DECLASSIFICATION/DOWNGRADING SCHEDULE												
16. DISTRIBUTION STATEMENT (of this Report) Approved for public release; distribution unlimited.														
17. DISTRIBUTION STATEMENT (of the abstract entered in Block 20, if different from Report)														
18. SUPPLEMENTARY NOTES														
19. KEY WORDS (Continue on reverse side if necessary and identify by block number) <table style="width: 100%; border-collapse: collapse;"> <tr> <td style="width: 33%;">Gripper</td> <td style="width: 33%;">Ammunition handling</td> <td style="width: 33%;">155-mm howitzer</td> </tr> <tr> <td>End effector</td> <td>Integrated Smart Artillery Synthesis</td> <td rowspan="3" style="vertical-align: middle; color: red;">IS AS</td> </tr> <tr> <td>End-of-arm tooling</td> <td>Design</td> </tr> <tr> <td>Robotic</td> <td>Hydraulic</td> </tr> <tr> <td>Artillery</td> <td>155-mm projectiles</td> </tr> </table>			Gripper	Ammunition handling	155-mm howitzer	End effector	Integrated Smart Artillery Synthesis	IS AS	End-of-arm tooling	Design	Robotic	Hydraulic	Artillery	155-mm projectiles
Gripper	Ammunition handling	155-mm howitzer												
End effector	Integrated Smart Artillery Synthesis	IS AS												
End-of-arm tooling	Design													
Robotic	Hydraulic													
Artillery	155-mm projectiles													
20. ABSTRACT (Continue on reverse side if necessary and identify by block number) A robotic gripper which picks up 155-mm projectiles and cylindrical propelling charges and holds them securely while they are moved through any orientation within a self-propelled howitzer is described. The exact tasks that the gripper must perform are studied and four preliminary concepts are shown. One concept is developed. The development effort includes a kinematic analysis, force analysis, stress analysis, and a complete drawing package.														

SECURITY CLASSIFICATION OF THIS PAGE(When Data Entered)

SECURITY CLASSIFICATION OF THIS PAGE(When Data Entered)

## CONTENTS

	Page
Introduction	1
Design Specifications	1
Gripper Concepts	2
General Design of Developed Concept	3
Gripping Force	4
Force Analysis	6
Kinematic Analysis	9
Stress Analysis	9
Piston Rationalization	21
Conclusions and Recommendations	23
References	25
Bibliography	25
Appendixes	
A Product Search	41
B Spatial Analysis	45
C Kinematic Analysis	59
D Drawings	75
Distribution List	101

## FIGURES

	Page
1 Integrated Smart Artillery Synthesis (ISAS) robotic demonstrator	27
2 Motion without tilt	28
3 Motion with tilt	28
4 Robot in flexed position	29
5 Three-piston gripper concept	29
6 Inflatable gasket gripper concept	30
7 Long-stroke concept	30
8 Short-stroke concept	31
9 Generalized gripper schematic	31
10 Worst case condition for gripping	32
11 Force analysis layout	32
12 Forces acting upon finger	33
13 Forces acting upon yoke	34
14 Forces acting upon yoke connector	34
15 Angular acceleration and acceleration of center of gravity of link 3 versus piston displacement	35
16 Pin locations	36
17 Stress locations on pin at point A	36
18 Stress locations on pin at point B	36
19 Stress locations on pin at point C	37
20 Stress locations on finger	37
21 Stress locations on yoke	38
22 Stress location on yoke connector	38
23 Stress locations on saddle	38

24	Curved beam analysis	39
25	"Pancake" hydraulic cylinder	40
26	ISAS robotic gripper	40

## INTRODUCTION

This report describes the development of a robotic gripper. Its function is to grasp and securely hold 6-inch-diameter (155-mm) projectiles and 6.25-inch-diameter modular propelling charges longitudinally about their center of gravity as they are moved through any orientation.

The gripper and its robotic arm are part of the Integrated Smart Artillery Synthesis (ISAS) project presently under development and will be installed in a modified M109 self-propelled howitzer (fig. 1). The robot transports the projectiles and charges from different locations within the howitzer and places them on an autoloader tray.

Most robotic systems which transport heavy loads keep them in an orientation parallel to the plane of the earth while permitting movement perpendicular to that plane (fig. 2). Several types of grippers are used to accomplish this task. One uses magnetic force; another employs pneumatic suction; a third utilizes mechanical force. A mechanical gripper may be hydraulically, pneumatically, or electrically powered.

Occasionally heavy loads must be moved through a variety of orientations. Generally, such loads are supported by bracing as shown in figure 3. Bracing permits rotation of up to 180 degrees out of a fixed plane of motion. An alternative method is to mechanically grasp the load with sufficient force to hold it securely in any plane. A third method makes use of a fixed frame containing an inflatable seal. When the seal is expanded, hydrostatic pressure holds the load in place.

## DESIGN SPECIFICATIONS

There are numerous specifications which the gripper must meet. For example, it must operate in a temperature range of 0 to 125°F. It must be weatherproof, but not necessarily waterproof. It must also be capable of operating in environments containing high levels of dust and dirt.

The maximum size of the gripper is determined by the space envelope available. The projectile rack configuration is such that a gripper may not be more than 9 inches wide. The gripper will partially encircle a projectile at its center of gravity in the area between the rotating bands and the bourrelet (fig. 4). The length of the gripper (distance from the outer edge of one finger to the outer edge of the other) may not exceed 8 inches.

For determining the gripper's height profile, the working area can be divided into two parts; that above the centerline of the projectile and that below the centerline. Dimensions above the centerline of the projectile are governed by the configuration of the robot. A representation of the robot in its flexed position holding a projectile is shown in figure 4. The gripper illustrated is an early concept. The projectile's centerline must be approximately 15

inches below the robot's lower joint to avoid interference. The design parameter is such that the gripper must fit between the middle section of the robot arm and the projectile when the robot is in this configuration.

The gripper will weigh approximately 30 pounds. It will be hydraulically powered by a system developing 2,000 psi operating pressure. The gripper must have sufficient holding force to permit transporting projectiles and charges in any attitude. The length of the robot arm may not exceed 43 inches. The robot's rotating joints will have a maximum angular velocity of 90 degrees per second. The x-y gantry to which the robot is attached will have a maximum traversing speed of 15 inches per second in both the x and y directions. The robot must be capable of stopping in 0.1 second. These specifications are used to calculate holding force requirements.

The gripper must also contain a feature which will operate a latch to release projectiles and charges from their racks. The exact position of the latches on the racks will be determined during the gripper's final design.

### GRIPPER CONCEPTS

Prior to development of the gripper concepts, known types were studied. Magnetic grippers were ruled out because the propelling charges they would be transporting are nonmagnetic. Pneumatic grippers were rejected because the available power source is hydraulic. A product search was conducted but no suitable gripper was found. Results of this investigation are described in appendix A.

In view of the nonavailability of a commercial product, an in-house concept study was initiated. Four design approaches were used.

The first design is shown in figure 5. This gripper consists of two U-shaped members, each containing three pistons. After the gripper is placed around the load, hydraulic pressure is applied to the pistons. The relative displacement of each piston is then measured and the robot automatically corrects its position to center the load. Once the load is centered, two valves are automatically closed to fix each piston in position. The accuracy of the robot when grasping its load is not critical because the gripper contains a positioning feedback system. This concept is easy to maintain since the readily accessible pistons are its only repair parts.

There are, however, disadvantages to this design. The position sensors required for the feedback system are costly. The pressure exerted upon the projectiles and charges is high, since the contact area is small. The gripper's required thickness, as determined by piston expansion, would probably exceed the desired space envelope. Also, in this application the force reactions on each piston are unusual in that they are not parallel to the piston's stroke. Therefore, the pistons will probably not be available as off-the-shelf items.

The second concept is shown in figure 6. This configuration is similar to the first concept but uses hydraulically inflatable gaskets in lieu of pistons. In this application, the shape of the gaskets is critical. If not properly shaped, they will permit the load to shift downward. When this occurs, fluid will flow through the gaskets causing them to expand above the centerline of the load. This will result in dropping the load. Presray Corporation fabricates inflatable gaskets which are capable of exerting the required force. They are also compatible with MIL-H-6083 hydraulic fluid. These gaskets, however, do not possess the shear strength required to hold the load.

The third concept, shown in figure 7, was devised following a study of available hydraulic actuators. Because hydraulics are usually associated with large items, most off-the-shelf actuators are too big or too heavy. However, Bimba Manufacturing Company makes a hydraulic cylinder 0.625 inch in diameter and 5 inches long with a 4-inch stroke. In this concept, when the cylinder is actuated, link two slides along the ground link, closing link three. As in the previous concepts, two gripper assemblies are required. This mechanism's greatest attribute is that it uses an off-the-shelf actuator; however, it requires a large space envelope.

The fourth concept evolved from the third concept. It was recognized that if link two of the third concept (fig. 7) were reshaped and driven from the sliding point, it would result in a more compact, efficient design. This fourth concept (fig. 8) requires the use of a different type actuator. A rotary actuator driving a cam was evaluated and discarded as being too heavy. However, the mechanism could also be driven by a linear actuator. Research has revealed that Fabco-Air, Inc. manufactures such an actuator. This company offers a line of pneumatic short-stroke "pancake" cylinders which could be used with low pressure hydraulics (under 500 psi nonshock).

Since the fourth concept appeared feasible, it was chosen for development.

#### GENERAL DESIGN OF DEVELOPED CONCEPT

Of the concepts previously described, the fourth was developed by computer program to determine the link lengths that would fit within the space envelope. The analysis, the program, and the program's output are described in appendix B.

As shown in appendix B, figure B-1, the distance between the center line of the mechanism and the lower left-hand pin (R) was varied from 3.3 inches to 4.5 inches in 0.1-inch increments. The distance between the center pivot point and the low end of the piston's stroke (S) was varied from 0.3-inch to 1.5 inches in 0.1-inch increments. The distance between the center line of the mechanism and the low end of the piston's stroke (D) was varied from 4 inches to 5.3 inches in 0.1-inch increments. The transmission angle ( $\theta$ ) of the closed linkage was fixed at 95 degrees. The initial transmission angle was varied from 121 degrees to 135 degrees in 1-degree increments. The longitudinal distance between the center line of the projectile and lower left-hand (Y) was fixed at 1 inch.

It was found that the space claim of this design did not exceed the space envelope. The program checked 35,490 linkages and found 195 desirable linkages.

Trends were studied, layout drawings were prepared, and a new generalized shape was conceived (fig. 9). This gripper appears to meet the design criteria.

### GRIPPING FORCE

The gripper must overcome dynamic as well as static loads. These forces may be additive and cause the load to slip from the gripper. Therefore, the normal force ( $N$ ) produced by the gripper must be sufficient to overcome slipping.

The robot arm's most critical orientation is illustrated in figure 10. In this instance, the robot is stopped while in full swing. The linear impulse, caused by stopping the arm, and the weight of the projectile are additive. (The angular impulse resulting from stopping the rotation of the projectile is comparatively small and is ignored.)

The linear impulse ( $\bar{F}_i$ ) can be approximated by the following relationship:

$$\bar{F}_i = \frac{\bar{V}_i - \bar{V}_o}{t} \frac{W}{g} \quad (1)$$

where

$V_i$  = Initial velocity of projectile (in./sec)

$V_o$  = Final velocity of projectile (in./sec)

$W$  = Weight of projectile (lb)

$t$  = Change in time (sec)

$g$  = Gravitational constant = 386.4 (in./sec<sup>2</sup>)

The initial velocity is the cross product of the angular velocity ( $\omega$ ) of the robot arm with the distance ( $r$ ) between the center of the arm's rotation and the center line of the projectile. Since the impulse force vector and the load vector are in the same direction, vector notation is dropped. When it is known that the maximum angular velocity of the arm is  $\pi/2$  rad/sec, and the distance ( $r$ ) is 48 inches, initial velocity can be calculated as

$$V_i = \omega r \quad (2)$$

$$V_i = \left(\frac{\pi}{2} \frac{\text{rad}}{\text{sec}}\right) (48.0 \text{ in.})$$

$$V_i = 75.4 \text{ in./sec}$$

Since the final  $\omega$  is zero,  $V_o$  is zero. The weight of the heaviest projectile is 103.4 pounds. The robot must stop within 0.1 second. This is the worst-case stop for the robot, so  $t$  is assumed to be 0.1 second. The linear impulse can now be calculated by equation 1.

$$F = \frac{(75.4 \text{ in./sec} - 0 \text{ in./sec}) (103.4 \text{ lb})}{(0.1 \text{ sec}) (386.4 \text{ in./sec}^2)} \quad (3)$$

$$F_i = 201.8 \text{ lb}$$

The total weight ( $F_T$ ) is the sum of the impulse force and the projectile's weight.

$$F_T = 201.8 \text{ lb} + 103.4 \text{ lb} \quad (4)$$

$$F_T = 305.2 \text{ lb}$$

The friction force ( $f$ ) between the gripper and the projectile must, as a minimum, equal  $F_T$ .

$$f = F_T \quad (5)$$

$$f = 305.2 \text{ lb}$$

When the gripper is holding the projectile, the normal force ( $N_p$ ) produced must equal the quotient of the friction force ( $f$ ) and the coefficient of friction between the two surfaces ( $\mu$ ).

$$N_p = \frac{f}{\mu} \quad (6)$$

The coefficient of dynamic friction between steel and paint is approximately 0.35. Since this is the minimum normal force required, a 10% safety factor is used.

$$N_p = \frac{305.2 \text{ lb}}{0.35} (1.1) \quad (7)$$

$$N_p = 959 \text{ lb}$$

The normal force needed to hold the charge ( $N_c$ ) can be calculated in the same manner. The weight of the charge is 30 pounds, and the coefficient of friction is 0.4. When the same procedure is used,  $N_c$  is 243.5 pounds.

In the following sections, the maximum forces and stresses acting upon the components of the gripper are studied. Since  $N_p$  is greater than  $N_c$ , the computations are based upon the requirements for  $N_p$ .

## FORCE ANALYSIS

The forces acting upon the gripper are greatest when the arm is rotating and the projectile is parallel to the ground. Vector forces added to the minimum normal force required to hold the projectile include the weight of the projectile and the dynamic force from the normal component of the projectile's acceleration. Since the forces resulting from the normal acceleration and the weight of the projectile ( $W$ ) are in the same direction, vector notation is omitted. The normal acceleration ( $a_n$ ) can be calculated using the following relation:

$$a_n = \omega^2 r \quad (8)$$

From this, the normal force is calculated.

$$F_n = \frac{a_n W}{g} \quad (9)$$

$$F_n = \frac{\omega^2 r W}{g}$$

$$F_n = \frac{\left(\frac{\pi}{2} \frac{\text{rad}}{\text{sec}}\right)^2 (48 \text{ in.}) (103.4 \text{ lb})}{(386.4 \text{ in./sec}^2)}$$

$$F_n = 31.7 \text{ lb}$$

The maximum force (FTP) attributable to the projectile is the sum of the dynamic force and its static weight.

$$FTP = F_n + W \quad (10)$$

$$FTP = 31.7 \text{ lb} + 103.4 \text{ lb}$$

$$FTP = 135.1 \text{ lb}$$

The gripper has four fingers, so the additional force ( $F_e$ ) on each will be one quarter the total added force.

$$F_e = 0.25 \text{ FTP} \quad (11)$$

$$F_e = 0.25 (135.1 \text{ lb})$$

$$F_e = 33.8 \text{ lb}$$

The minimum normal force on each finger remains at 959 pounds, since friction is not a function of area (number of fingers). With the layout in figure 11, the maximum normal force ( $N$ ) is the vector sum of the minimum normal force and the weight of the load.

$$N = N_p + Fe \cos 52^\circ \quad (12)$$

$$N = 959 \text{ lb} + 33.8 \text{ lb} \cos 52^\circ$$

$$N = 980 \text{ lb}$$

Each gripper makes 3-point contact with its load. By summing the forces in the y direction, the reaction force (R) can be calculated.

$$\Sigma F_y = 0 \quad (13)$$

$$R + FT_p (0.5) - 2N \sin 38^\circ = 0$$

$$R = -FT_p (0.5) + 2N \sin 38^\circ$$

$$R = -135.1 \text{ lb} (0.5) + 2 (980 \text{ lb}) \sin 38^\circ$$

$$R = 1,139 \text{ lb}$$

The internal forces of the gripper can now be calculated. Starting with the finger (fig. 12), moments can be summed about point C to determine the magnitude of FAB.

$$\Sigma M_C = 0 \quad (14)$$

$$2.387 \text{ in. } F_{AB} \cos 17^\circ - 3.25 \text{ in. } N \cos 38^\circ - 1.7 \text{ in. } N \sin 38^\circ = 0$$

$$F_{AB} = \frac{N (3.25 \text{ in. } \cos 38^\circ + 1.7 \text{ in. } \sin 38^\circ)}{2.387 \text{ in. } \cos 17^\circ}$$

$$F_{AB} = \frac{980 \text{ lb} (3.25 \text{ in. } \cos 38^\circ + 1.7 \text{ in. } \sin 38^\circ)}{2.387 \text{ in. } \cos 17^\circ}$$

$$F_{AB} = 1,549 \text{ lb}$$

Once FAB is known, Cx, Cy, the magnitude of C, and its direction from the x axis ( $\beta$ ), can be determined by summing the forces in the X and Y directions.

$$\Sigma F_x = 0 \quad (15)$$

$$Cx - F_{AB} \cos 17^\circ - N \cos 38^\circ = 0$$

$$Cx = F_{AB} \cos 17^\circ + N \cos 38^\circ$$

$$Cx = 1,549 \text{ lb} \cos 17^\circ + 980 \text{ lb} \cos 38^\circ$$

$$Cx = 2,253 \text{ lb}$$

$$\Sigma F_y = 0 \quad (16)$$

$$C_y - F_{AB} \sin 17^\circ - N \sin 38^\circ = 0$$

$$C_y = F_{AB} \sin 17^\circ + N \sin 38^\circ$$

$$C_y = 1,549 \text{ lb} \sin 17^\circ + 980 \text{ lb} \sin 38^\circ$$

$$C_y = 1,056 \text{ lb}$$

$$|C| = (C_x^2 + C_y^2)^{1/2} \quad (17)$$

$$|C| = [(2,254 \text{ lb})^2 + (1,056)^2]^{1/2}$$

$$|C| = 2,489 \text{ lb}$$

$$\beta = \tan^{-1} \frac{C_y}{C_x} \quad (18)$$

$$\beta = \tan^{-1} \frac{1,056 \text{ lb}}{2,253 \text{ lb}}$$

$$\beta = 25^\circ$$

Also, once  $F_{AB}$  is known, the forces on the yoke (fig. 13) can be determined. Since there are two forces at the finger connection, each will be one half  $F_{AB}$ , or 775 pounds. When the forces along the yoke are summed,  $F_{BA}$  must equal  $F_{AB}$  in magnitude and be opposite in direction. Since one of the forces at the yoke's finger connection is offset from the other two forces, it produces a force perpendicular to the yoke at the piston connection. From the sum of the moments about B, the magnitude of this force can be determined.

$$\Sigma M_B = 0 \quad (19)$$

$$F_{BAZ} - \frac{F_{AB}}{2} (0.3) = 0$$

$$F_{BAZ} = F_{AB} (0.15)$$

$$F_{BAZ} = 1,549 \text{ lb} (0.15)$$

$$F_{BAZ} = 232 \text{ lb}$$

Since  $F_{BA}$  is known, the forces in the yoke connector (fig. 14) can now be determined. A torque ( $T$ ) will be present on the connector from the two offset  $F_{BA}$  forces.

$$T = 0.75 \text{ FBA} \quad (20)$$

$$T = (0.75) (1,549 \text{ lb})$$

$$T = 1,162 \text{ in.-lb}$$

This torque will cause stress in the end posts. The maximum compression force ( $F$ ) which the piston must produce can now be solved.

$$F = 2 \text{ FBA} \sin 17^\circ \quad (21)$$

$$F = 2 (1,549 \text{ lb}) \sin 17^\circ$$

$$F = 906 \text{ lb}$$

It must be remembered that this maximum compression force includes dynamic forces. When an analysis excluding the dynamic forces is performed, the initial force which the piston produces is 886 pounds.

A similar analysis can be completed for gripping a charge. The result is that the piston will have a working force of 225 pounds and a maximum force of 234 pounds.

### KINEMATIC ANALYSIS

A kinematic analysis of the mechanism was conducted to determine if the dynamic forces of the moving links should be included. The gripper was modeled as an offset slider crank mechanism. The velocity of the piston was assumed constant since acceleration, once the mechanism is moving, is approximately zero. Position, velocity, and acceleration of different points on the mechanism were calculated as a function of piston velocity. The analysis, the program, and a sample program output are shown in appendix C.

The angular acceleration and the acceleration of the center of gravity of link R3 for a closing time of 1 second are shown in figure 15. The linear and angular accelerations for link R2 are of the same magnitude. Since the accelerations are small and the crank is almost balanced, the forces stemming from the movement of the links are not included.

### STRESS ANALYSIS

This section provides details of the stress analysis of the various components of the gripper. The pins at points A, B, and C are detailed in figure

16. The pin at point A is in single shear at two places (fig. 17). Due to symmetry, the shear stresses ( $\tau$ ) are equal at both shear points. For circular cross sections, the maximum shear stress is at the center and can be calculated as:

$$\tau_{\max} = \frac{16 FBA}{3 \pi d^2} \quad (22)$$

For the pin at point A,

$$\tau_{\max} = \frac{16 (1,549 \text{ lb})}{3 \pi (0.3125 \text{ in.})^2} \quad (23)$$

$$\tau_{\max} = 27,000 \text{ psi}$$

The maximum shear stress theory, which is used throughout the design, states that the maximum yield strength ( $S_y$ ) should be at least twice the maximum shear stress, or

$$S_y \text{ min} = 2 \tau_{\max} \quad (24)$$

For the pin at point A,

$$S_y \text{ min} = 2 (27,000 \text{ psi}) \quad (25)$$

$$S_y \text{ min} = 54,000 \text{ psi}$$

The material used to make the pins has a yield strength of 120,000 psi. The factor of safety (FS) is the ratio of the yield strength to the minimum required yield strength.

$$FS = \frac{S_y}{S_y \text{ min}} \quad (26)$$

For the pin at point A,

$$FS = \frac{120,000 \text{ psi}}{54,000 \text{ psi}} \quad (27)$$

$$FS = 2.2$$

The pin at point B is in double shear with the same force as the pin at point A but has a smaller diameter (fig. 18). For a pin in double shear, the maximum shear stress will be half that of a pin in single shear.

$$\tau_{\max} = \frac{8FAB}{3 \pi d^2} \quad (28)$$

For the pin point at B,

$$\tau_{\max} = \frac{8 (1,549 \text{ lb})}{3 \pi (0.25 \text{ in.})^2} \quad (29)$$

$$\tau_{\max} = 21,000 \text{ psi}$$

The minimum yield strength and factor of safety can be calculated using equations 24 and 26, respectively:

$$S_y_{\min} = 2 \tau_{\max} \quad (24)$$

$$S_y_{\min} = 2 (21,000 \text{ psi}) \quad (30)$$

$$S_y_{\min} = 42,000 \text{ psi}$$

$$FS = \frac{S_y}{S_y_{\min}} \quad (26)$$

$$FS = \frac{120,000 \text{ psi}}{42,000 \text{ psi}} \quad (31)$$

$$FS = 2.9$$

The pin at point C (fig. 19) is also in double shear. The pin's maximum shear stress, minimum yield strength, and factor of safety can be calculated by equations 28, 24, and 26, respectively:

$$\tau_{\max} = \frac{8 F_c}{3 \pi d^2} \quad (28)$$

$$\tau_{\max} = \frac{8 (2,489 \text{ lb})}{3 \pi (0.25 \text{ in.})^2} \quad (32)$$

$$\tau_{\max} = 33,800 \text{ psi}$$

$$S_y_{\min} = 2 \tau_{\max} \quad (24)$$

$$S_y_{\min} = 2 (33,800 \text{ psi}) \quad (33)$$

$$S_y \text{ min} = 67,600 \text{ psi}$$

$$FS = \frac{S_y}{S_y \text{ min}} \quad (26)$$

$$FS = \frac{120,000 \text{ psi}}{67,600 \text{ psi}} \quad (34)$$

$$FS = 1.8$$

The next component discussed is the finger (fig. 20), since its dimensions are critical to the design of other pieces. The distance between B and C as well as the shape of the curved portion was determined by the working area and the conceptual analysis of the mechanism. The cross sectional area was determined by the strength requirements. The stress and strength calculations for three of the critical sections are presented here. Section B'-B' has bearing stress imparted by the pin as well as a shear (tear out) stress. The bearing stress ( $\sigma$ ) can be approximated by the following relationship:

$$\sigma = \frac{F_{AB}}{t d} \quad (35)$$

where

$t$  = thickness of section (in.)

$d$  = diameter of hole (in.)

For this section,  $t$  is 0.5 inch and  $d$  is 0.25 inch. There are two components to the bearing stress at this point,  $\sigma_x$ , and  $\sigma_y$ . They can be calculated using equation 35.

$$\sigma_x = \frac{-1,549 \text{ lb cos } 17^\circ}{(0.5 \text{ in.})(0.25 \text{ in.})} \quad (36)$$

$$\sigma_x = -11,800 \text{ psi}$$

$$\sigma_y = \frac{-1,549 \text{ lb sin } 17^\circ}{(0.5 \text{ in.})(0.25 \text{ in.})} \quad (37)$$

$$\sigma_y = -3,600 \text{ psi}$$

The minus notation refers to a compressive stress.

The shear stress acts only through the left-hand portion of the cross section. For a rectangular cross section, the maximum shear stress is at the center and can be calculated using the following relationship:

$$\tau = \frac{3}{2} \frac{F_{AB}}{A} \quad (38)$$

where

$$A = \text{cross sectional area (in.}^2\text{)}.$$

in.<sup>2</sup> Since the shear stress acts only through the left-hand section, A is 0.24

$$\tau_{xy} = \frac{3}{2} \frac{(1,549 \text{ lb}) \cos 17^\circ}{0.24 \text{ in.}^2} \quad (39)$$

$$\tau_{xy} = 9,260 \text{ psi}$$

With the use of Mohr's circle maximum shear stress can be calculated from the individual stresses using the following relationship:

$$\tau_{max} = \left( \left( \frac{\sigma_x - \sigma_y}{2} \right)^2 + \tau_{xy}^2 \right)^{1/2} \quad (40)$$

For this section,

$$\tau_{max} = \left( \left( \frac{-11,800 \text{ psi} - (-3,600 \text{ psi})}{2} \right)^2 + (9,260 \text{ psi})^2 \right)^{1/2} \quad (41)$$

$$\tau_{max} = 10,100 \text{ psi}$$

With the use of equation 24, the minimum yield strength can be determined.

$$Sy_{min} = 2 \tau_{max} \quad (24)$$

$$Sy_{min} = 2 (10,100 \text{ psi}) \quad (42)$$

$$Sy_{min} = 20,200 \text{ psi}$$

The finger has a minimum yield strength of 120,000 psi. The factor of safety for this cross section can now be solved using equation 26.

$$FS = \frac{Sy}{Sy_{min}} \quad (26)$$

$$FS = \frac{120,000 \text{ psi}}{20,200 \text{ psi}} \quad (43)$$

$$FS = 5.9$$

The most critical stresses are at section C'-C'. They include a bearing stress from the pin, a bending stress due to the moment, and a shear stress. The bearing stress is almost constant throughout the right-hand side. The bending moment increases from the center to a maximum tensile stress at the right outer edge. The shear stress is a parabolic function which is zero at the edge of the hole and at the outer edge of the section with maximum stress halfway between. The effect of the bending stress is greater than that of the shear stress. For this reason, the stresses at the right outer edge are analyzed.

As reported in reference 1, the maximum tensile stress will be twice what it would be were the hole not present. This is true for ratios of hole diameter to width less than 5. From this, it is evident that the tensile stress at the edge of the hole can be calculated from the following:

$$\sigma_y = \frac{6M}{t D^2} \quad (44)$$

where

M = Moment (in.-lb)

t = Thickness of section (in.)

D = Width of section (in.)

For the section to be studied,

$$M = 1,549 \text{ lb } (\cos 17^\circ) \times 2.387 \text{ in.} = 3,686 \text{ in.-lb}$$

$$t = 1.0 \text{ in.}$$

$$D = 1.2 \text{ in.}$$

$$\sigma_y = \frac{6 (3,686 \text{ in.-lb})}{(1.0 \text{ in.}) (1.2 \text{ in.})^2} \quad (45)$$

$$\sigma_y = 15,400 \text{ psi}$$

The compressive stress in the x direction can be calculated using equation 35 and a value of 2253 pounds for Cx.

$$\sigma_x = \frac{Cx}{t d} \quad (35)$$

$$\sigma_x = \frac{2,253 \text{ lb}}{(0.48 \text{ in.})(0.25 \text{ in.})} \quad (46)$$

$$\sigma_x = -18,775 \text{ psi}$$

The shear stress in the x-y direction is zero at this point, so the maximum shear stress can be calculated using equation 40.

$$\tau_{\max} = \left( \left( \frac{\sigma_x - \sigma_y}{2} \right)^2 + \tau_{xy}^2 \right)^{1/2} \quad (40)$$

$$\tau_{\max} = \left( \left( \frac{18,775 \text{ psi} - 15,400 \text{ psi}}{2} \right)^2 \right)^{1/2} \quad (47)$$

$$\tau_{\max} = 17,100 \text{ psi}$$

Equations 24 and 26 may now be used to calculate the minimum yield strength and the factor of safety at this section.

$$S_y_{\min} = 2 \tau_{\max} \quad (24)$$

$$S_y_{\min} = 2 (17,100 \text{ psi}) \quad (48)$$

$$S_y = 34,200 \text{ psi}$$

$$FS = \frac{S_y}{S_y_{\min}} \quad (26)$$

$$FS = \frac{120,000 \text{ psi}}{34,200 \text{ psi}} \quad (49)$$

$$FS = 3.5$$

The stress at section D'-D' is caused by bending and shear. Again, the stress is greatest at the inner edge. The tension stress due to bending can be calculated using the following relationship:

$$\sigma = \frac{M c}{I} \quad (50)$$

where

c = distance between neutral axis and point of calculation (in.)

I = moment of inertia (in.<sup>4</sup>)

The moment of inertia for a rectangular cross section is

$$I = \frac{1}{12} b h^3 \quad (51)$$

where

h = height of section (in.)

b = base of section (in.)

For this section,

$$b = 2.0 \text{ in.}$$

$$h = 0.7 \text{ in.}$$

The moment of inertia can be calculated using equation 52.

$$\begin{aligned} I &= \frac{1}{12} (2.0 \text{ in.}) (0.7 \text{ in.})^3 \\ I &= 0.057 \text{ in.}^4 \end{aligned} \quad (52)$$

The distance between the point of calculation and the neutral axis is 0.35 inch. The moment on this section is 2,058 inch-pounds. The tensile stress can now be calculated by substituting into equation 50.

$$\sigma_y = \frac{M c}{I} \quad (50)$$

$$\sigma_y = \frac{(2,058 \text{ in.-lb}) (0.35 \text{ in.})}{(0.057 \text{ in.}^4)} \quad (53)$$

$$\sigma_y = 12,600 \text{ psi}$$

There are no other stresses on this section, so equation 40 can be used to solve for the maximum shear stress.

$$\tau_{\max} = \left( \left( \frac{\sigma_x - \sigma_y}{2} \right)^2 + \tau_{xy} \right)^{1/2} \quad (40)$$

$$\tau_{\max} = \left( \left( \frac{-12,600 \text{ psi}}{2} \right)^2 \right)^{1/2} \quad (54)$$

$$\tau_{\max} = 6,300 \text{ psi}$$

The maximum yield strength and factor of safety can now be calculated.

$$S_y_{\min} = 2 \tau_{\max} \quad (24)$$

$$S_y_{\min} = 2 (6,300 \text{ psi}) \quad (55)$$

$$S_y_{\min} = 12,600 \text{ psi}$$

$$FS = \frac{S_y}{S_y_{\min}} \quad (26)$$

$$FS = \frac{120,000 \text{ psi}}{12,600 \text{ psi}} \quad (56)$$

$$FS = 9.5$$

The finger connects to the yoke by the pin at B (fig. 21). There is bearing stress at pins B and A. There is also a bending stress at section A'-A'. These are critical sections and are analyzed separately.

For calculation of the bearing stress at section B'-B', equation 35 can be used. The total contact area is used.

$$\sigma_x = \frac{F_{AB}}{t d} \quad (35)$$

$$\sigma_x = \frac{-1,549 \text{ lb}}{(0.5 \text{ in.})(0.25 \text{ in.})} \quad (57)$$

$$\sigma_x = -12,400 \text{ psi}$$

Again, equation 40 is used to calculate the maximum shear stress; however, since there is only one component, it reduces to the following:

$$\tau_{\max} = \pm \frac{\sigma}{2} \quad (58)$$

$$\tau_{\max} = \pm \frac{-12,400 \text{ psi}}{2} \quad (59)$$

$$\tau_{\max} = 6,200 \text{ psi}$$

For this section, the maximum shear stress is 6,200 psi. Since the shear strength of the yoke is 120,000 psi, the factor of safety is 19.4.

At section A'-A', t is 0.3 inch and d is 0.3125 inch. The bearing stress here is

$$\sigma_x = \frac{FAB}{t d} \quad (35)$$

$$\sigma_x = \frac{-1,549 \text{ lb}}{(0.3 \text{ in.}) (0.3125 \text{ in.})} \quad (60)$$

$$\sigma_x = -16,500 \text{ psi}$$

There is an added bending moment at A'-A' which can be calculated using equation 50. This has a rectangular cross section where

$$I = 0.001 \text{ in.}^4$$

$$C = 0.5 \text{ in.}$$

$$M = 51 \text{ in.-lb}$$

$$\sigma_y = \frac{Mc}{I} \quad (50)$$

$$\sigma_y = \frac{(51 \text{ in.-lb}) (0.5 \text{ in.})}{(0.001 \text{ in.}^4)} \quad (61)$$

$$\sigma_y = 25,500 \text{ psi}$$

There is no shear stress in the x-y plane, so the maximum shear stress at this section can now be calculated using equation 40.

$$\tau_{\max} = \left( \left( \frac{\sigma_x - \sigma_y}{2} \right)^2 + \tau_{xy}^2 \right)^{1/2} \quad (40)$$

$$\tau_{\max} = \left( \left( \frac{-16,500 \text{ psi} - 25,500 \text{ psi}}{2} \right)^2 \right)^{1/2} \quad (62)$$

$$\tau_{\max} = 21,000 \text{ psi}$$

Again, with the use of equations 24 and 26,  $Sy_{\min}$  is 42,000 psi and the FS is 2.9.

The yokes attach to the piston via a connector (fig. 22). There is a bearing stress in the pin resulting from the torque it must transmit. The maximum bearing stress is at A'-A' and can be calculated by equation 35. Assuming half the connecting area withstands the bearing stress imparted by one yoke,  $t$  is 0.2 inch.

$$\sigma = \frac{FAB}{t d} \quad (35)$$

$$\sigma = \frac{-1,549 \text{ lb}}{(0.5 \text{ in.})(0.25 \text{ in.})} \quad (63)$$

$$\sigma = -24,800 \text{ psi}$$

Combining equations 58 and 24,

$$Sy_{\min} = \sigma \quad (64)$$

$$Sy_{\min} = 24,800 \text{ psi}$$

The factor of safety can be solved using equation 26 with Sy having a value of 120,000 psi.

$$FS = \frac{Sy}{Sy_{\min}} \quad (26)$$

$$FS = \frac{120,000 \text{ psi}}{24,800 \text{ psi}} \quad (65)$$

$$FS = 4.8$$

The last item discussed is the saddle (fig. 23). Two critical sections are involved. First is the bearing and tearout area at C. Second is the combined bending and compression at section E'-E'.

The bearing stress at C can be calculated by equation 35.

$$\sigma_x = \frac{FC}{t d} \quad (35)$$

$$\sigma_x = \frac{2,489 \text{ lb}}{(1.0 \text{ in.})(0.25 \text{ in.})} \quad (66)$$

$$\sigma_x = 10,000 \text{ psi}$$

The tearout stress is in the y direction and is caused by the shear. Since this is a rectangular cross section, the maximum shear in the x-y direction can be calculated using equation 38. The area is 0.4 in.<sup>2</sup>.

$$\tau_{xy} = \frac{3}{2} \frac{FC}{A} \quad (38)$$

$$\tau_{xy} = \frac{3}{2} \frac{2,489 \text{ lb}}{0.4 \text{ in.}^2} \quad (67)$$

$$\tau_{xy} = 9,300 \text{ psi}$$

The maximum shear at this section can be calculated using equation 40.

$$\tau_{max} = \left( \left( \frac{\sigma_x - \sigma_y}{2} \right)^2 + \tau_{xy}^2 \right)^{1/2} \quad (40)$$

$$\tau_{max} = \left( \left( \frac{10,000 \text{ psi}}{2} \right)^2 + (9,300 \text{ psi})^2 \right)^{1/2} \quad (68)$$

$$\tau_{max} = 10,500 \text{ psi}$$

The minimum yield strength must be 21,200 psi. This results in a factor of safety of 5.6 since the material has a yield strength of 120,000 psi.

Section E'-E' (fig. 23) is a curved beam in bending. Equations 69 through 72 are taken from reference 2. The meaning of the symbols is shown in figure 24.

$$r_n = \frac{\sum A}{\sum \left( b \ln \left( \frac{r_o}{r_i} \right) \right)} \quad (69)$$

$$r_n = \frac{(1.2 \text{ in.}^2)}{2 \ln \left( \frac{3.725 \text{ in.}}{3.125 \text{ in.}} \right)} \quad (70)$$

$$r_n = 3.416 \text{ inches}$$

$$e = r_g - r_n \quad (71)$$

$$e = 3.425 \text{ in.} - 3.416 \text{ in.} \quad (72)$$

$$e = 0.009 \text{ inch}$$

The bending stress at the inner surface, which is the location of maximum stress, can now be calculated.

$$\sigma_i = \frac{M_{ci}}{A_e r_i} \quad (73)$$

$$\sigma_i = \frac{[(2,489 \text{ lb})(1.1 \text{ in.})](0.3 \text{ in.})}{(1.2 \text{ in.}^2)(0.009 \text{ in.})(3.125 \text{ in.})} \quad (74)$$

$$\sigma = 25,000 \text{ psi}$$

With equations 24 and 26,  $S_y_{min}$  is 50,000 psi and the factor of safety is 2.4.

### PISTON RATIONALIZATION

The piston must travel 1.6 inches between the mechanism's fully opened and fully closed positions. Since a piston should work only over 80% of its stroke, the stroke should be 2 inches. As shown in the Force Analysis section, the piston must produce forces of 906 pounds and 234 pounds.

The piston selected for this use is double acting and has a 1.63-inch bore with a 2-inch stroke (fig. 25).

The piston has a maximum pressure rating of 500 psi. Its operating pressures can be calculated as shown. Pressure ( $P$ ) is the force divided by area.

$$P = \frac{F}{A} \quad (75)$$

The area of the piston is

$$A = \frac{\pi d^2}{4} \quad (76)$$

where

$d$  = diameter of piston (1.625 in.)

$$A = \frac{\pi (1.625 \text{ in.})^2}{4} \quad (77)$$

$$A = 2.07 \text{ in.}^2$$

When gripping a projectile, the piston must have a working force of 886 pounds. The piston's pressure at this force will be

$$P_{wp} = \frac{886 \text{ lb}}{2.07 \text{ in.}^2} \quad (78)$$

$$P_{wp} = 427 \text{ psi}$$

To properly grip a charge, the piston must produce a working force of 225 pounds. The piston's pressure at this force will be

$$P_{wc} = \frac{225 \text{ lb}}{2.07 \text{ in.}^2} \quad (79)$$

$$P_{wc} = 109 \text{ psi}$$

Due to dynamic forcing, the maximum force could be as much as 906 pounds. The pressure at this force level is

$$P_{max} = \frac{906 \text{ lb}}{2.07 \text{ in.}^2} \quad (80)$$

$$P_{max} = 438 \text{ psi}$$

Note that  $P_{max}$  is less than the 500 psi rating of the piston.

## CONCLUSIONS AND RECOMMENDATIONS

The gripper introduced meets all the specifications detailed in this report. The gripper was designed to the dimensions of the largest object to be grasped; namely, the largest proposed dimension of the experimental uni charge.\* After the dimensions of the uni charge are known, the gripper should be retooled to the dimensions of the largest object it must then grasp. This will not only result in a better grasp of a load, but will also reduce the stresses within the gripper.

Drawings of the gripper as presently configured are shown in appendix D. An artist's conception of the gripper precisely tooled to the contour of a projectile is shown in figure 26.

---

\* The uni charge is a rigid-case propelling charge presently under development.

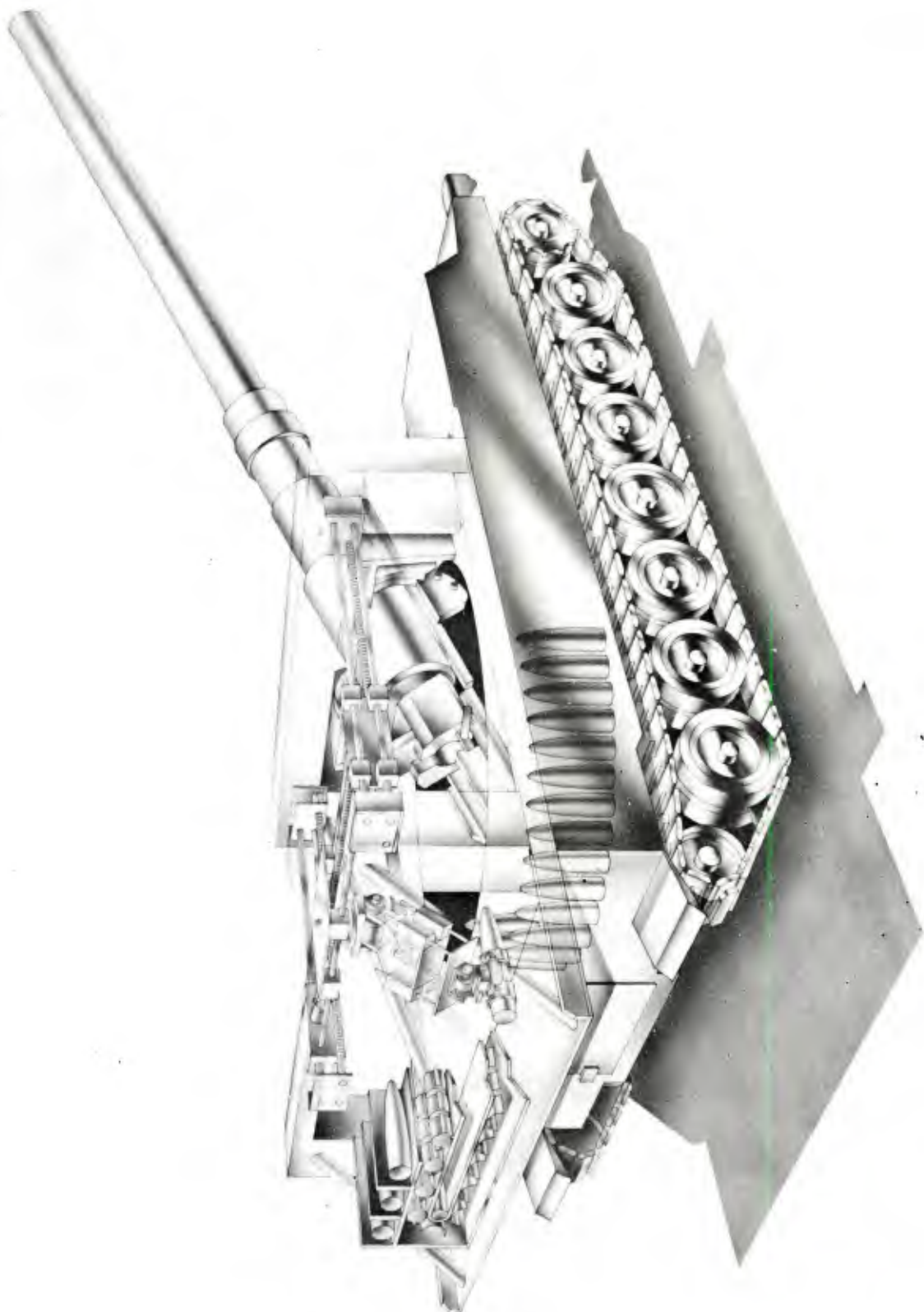
## REFERENCES

1. R. B. Heywood, Designing by Photoelasticity, Adland and Son, Ltd., Great Britain, 1952.
2. Omer W. Blodgett, Design of Weldments, The James F. Lincoln Arc Welding Foundation, Cleveland, Ohio, 1963.

## BIBLIOGRAPHY

1. Ferdinand P. Beer and E. Russell Johnston, Jr., Mechanics of Materials, McGraw-Hill Book Co., New York, 1981.
2. Dimensioning and Tolerancing: ANSI Y14.5M, American Society of Mechanical Engineers, New York, 1983.
3. J. Kammerer, 155MM Artillery Weapon Systems Reference Data Book, U.S. Army Armament Research and Development Command, Dover, NJ, 1980.
4. Erik Oberg and F. D. Jones, Machinery's Handbook: For Machine Shop and Drafting Room, fourteenth edition, The Industrial Press, New York, 1949.
5. Raymond J. Roark and Warren C. Young, Formulas for Stress and Strain, fifth edition, McGraw-Hill Book Co., New York, 1975.
6. Ryerson Stocks and Services Catalogue, Joseph T. Ryerson and Son, Inc., Jersey City, NJ, 1980.
7. Joseph Edward Shigley and John Joseph Uicker, Jr., Theory of Machines and Mechanisms, McGraw-Hill Book Co., New York, 1980.

Figure 1. Integrated Smart Artillery Synthesis (ISAS) robotic demonstrator



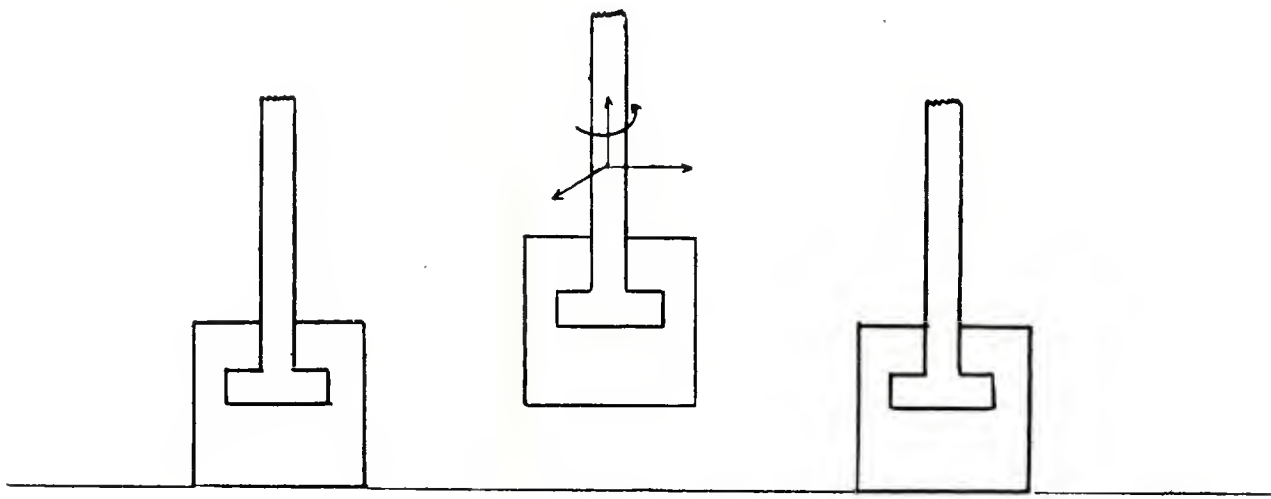


Figure 2. Motion without tilt

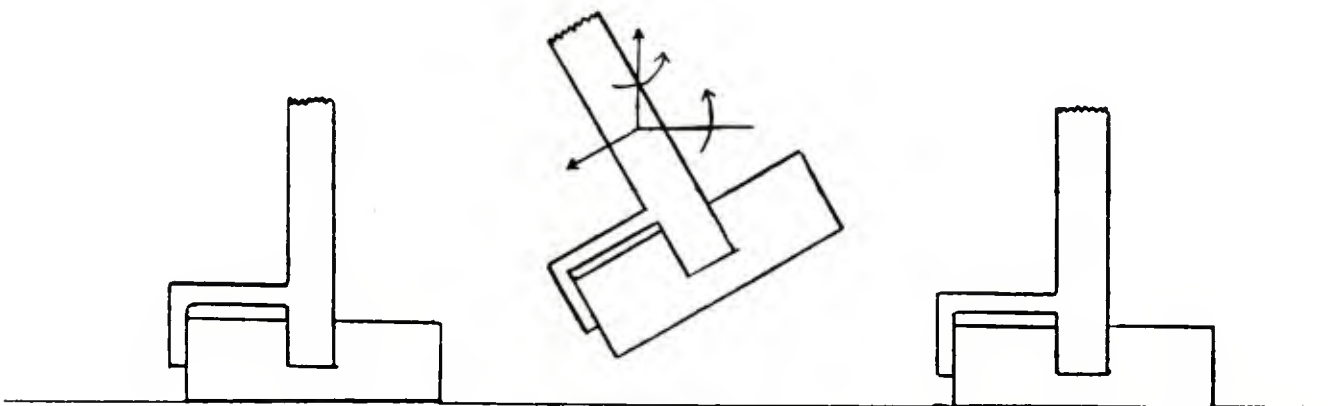


Figure 3. Motion with tilt

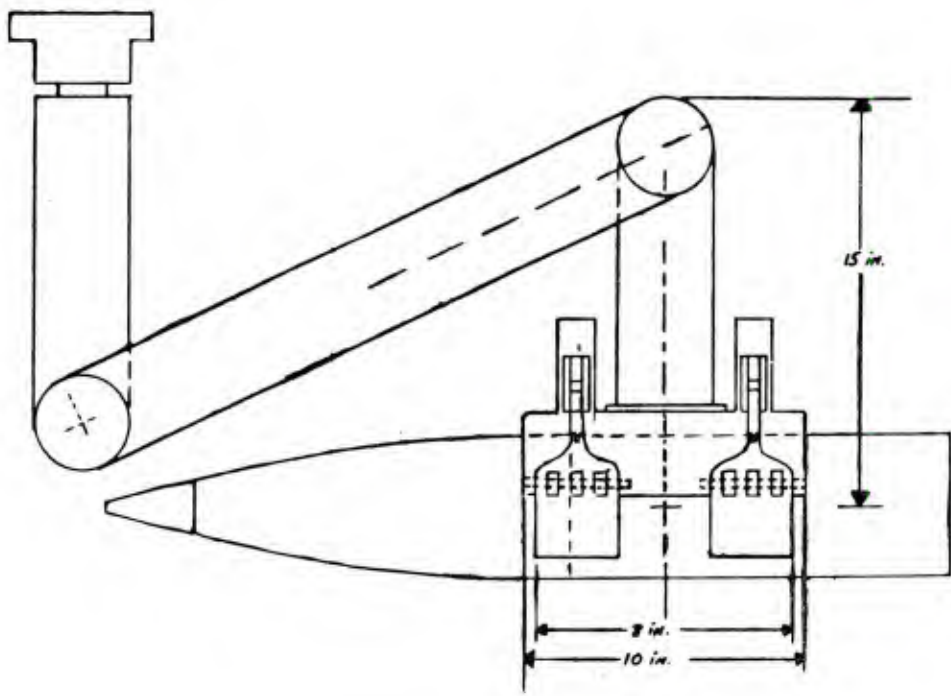


Figure 4. Robot in flexed position

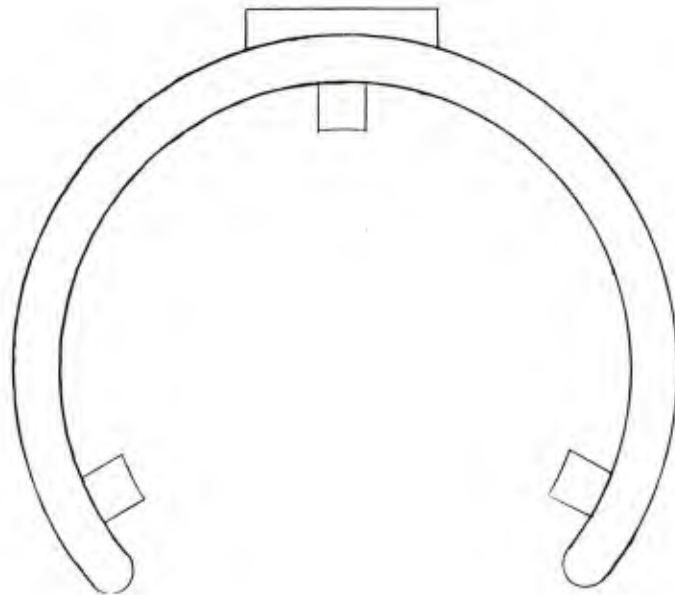


Figure 5. Three-piston gripper concept

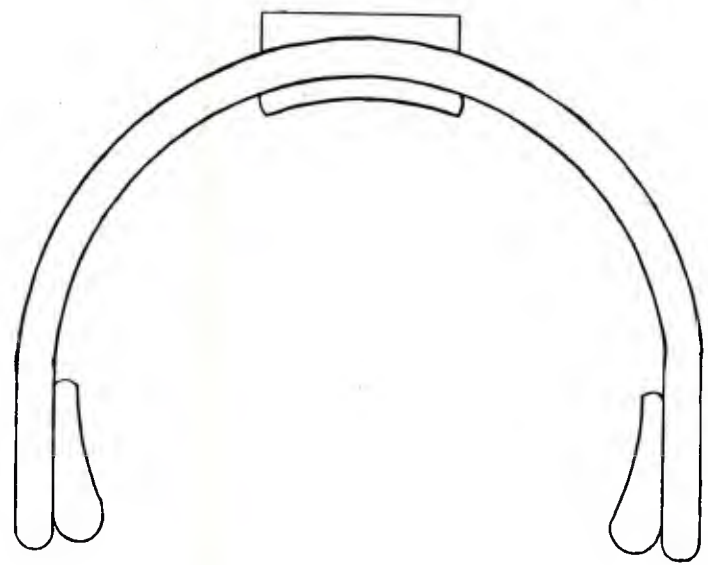


Figure 6. Inflatable gasket gripper concept

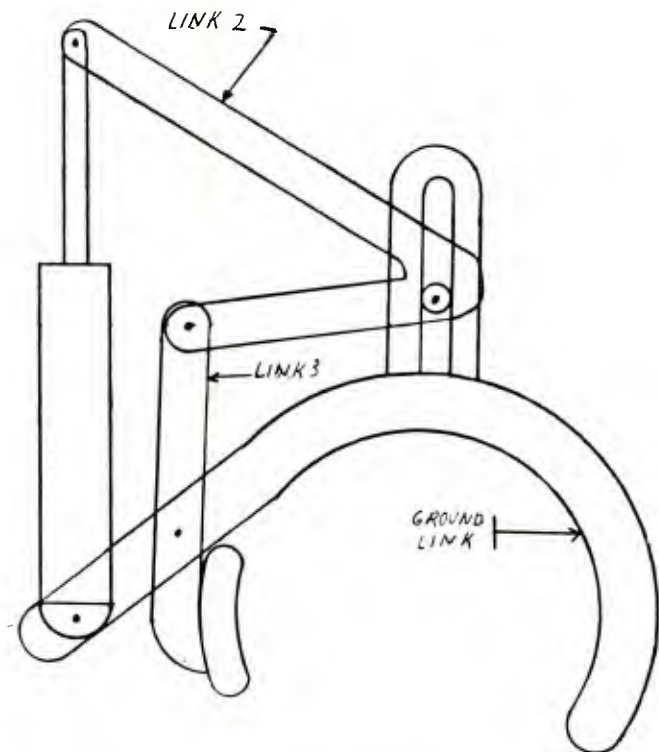


Figure 7. Long-stroke concept

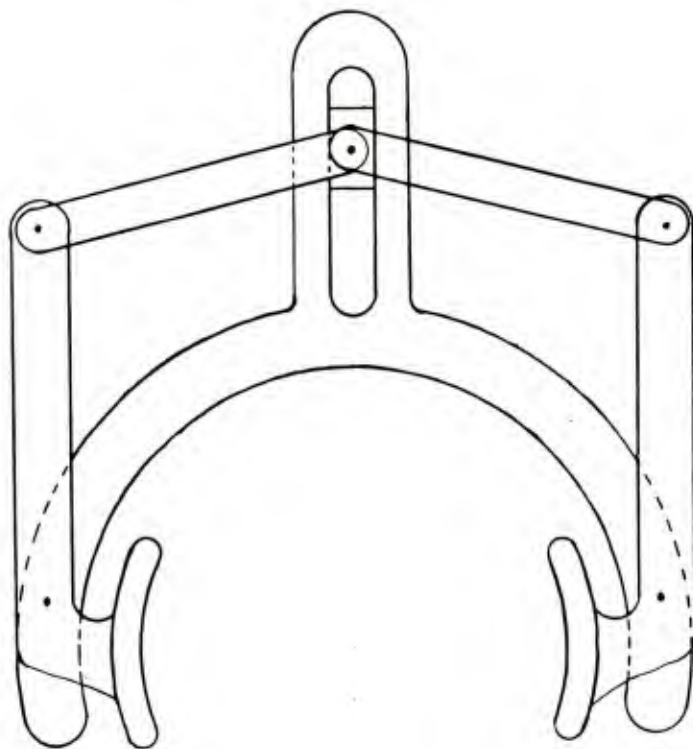


Figure 8. Short-stroke concept

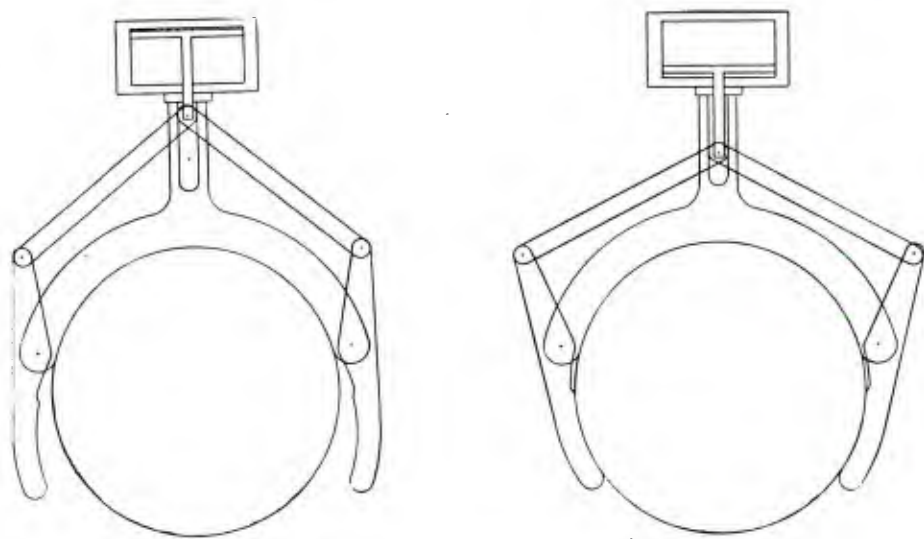


Figure 9. Generalized gripper schematic

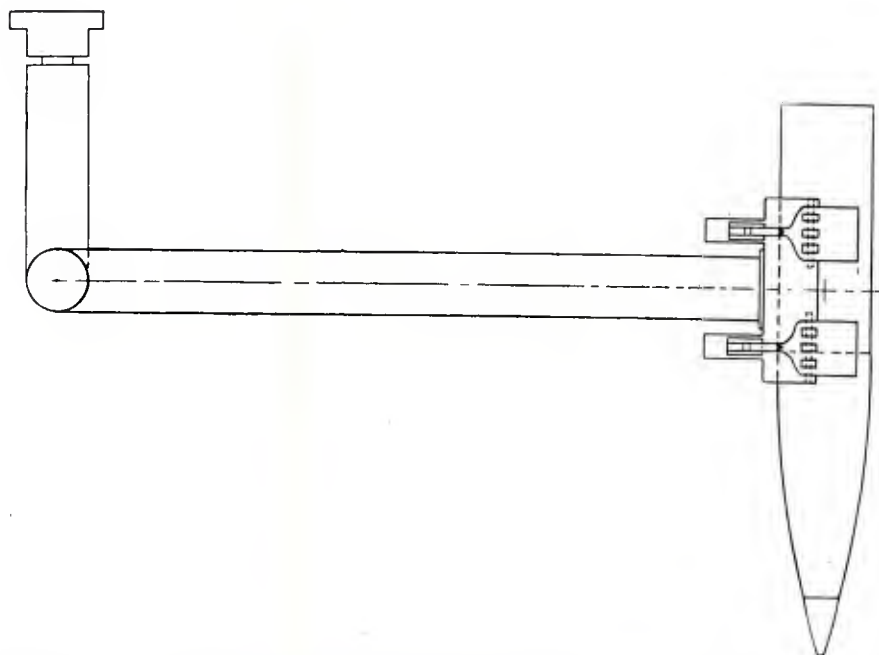


Figure 10. Worst case condition for gripping

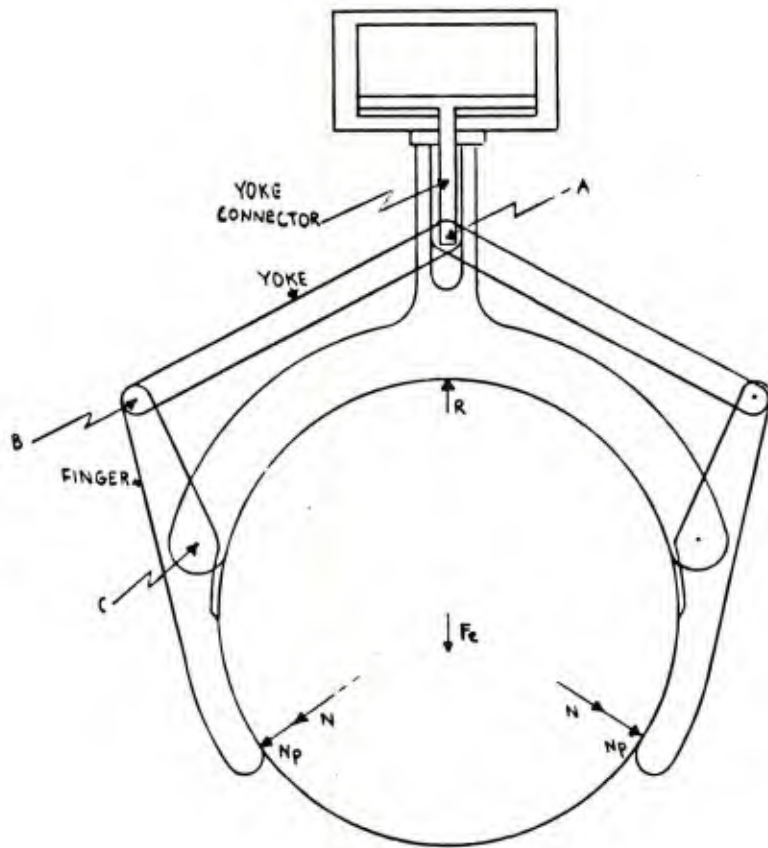


Figure 11. Force analysis layout

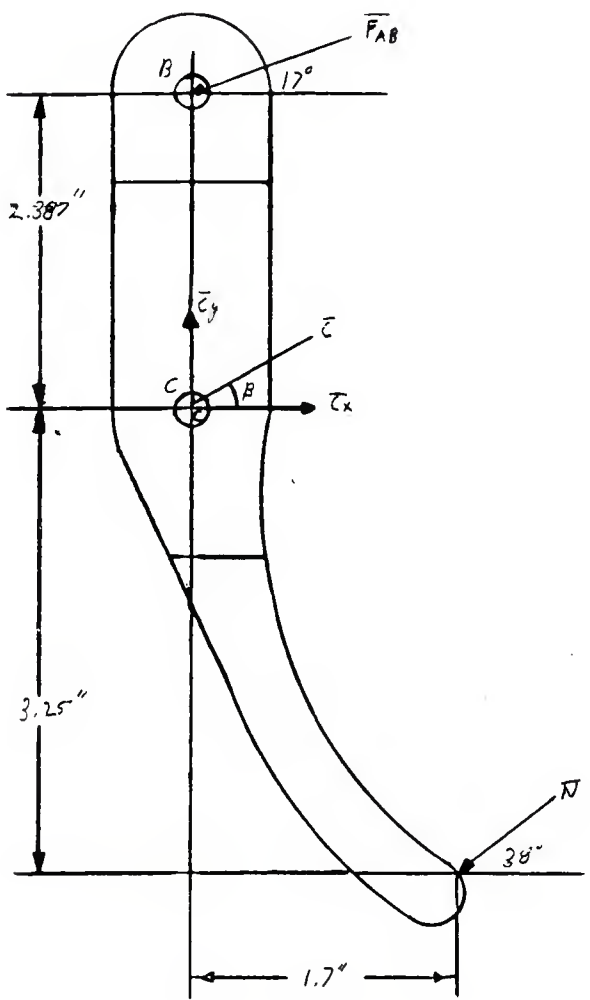


Figure 12. Forces acting upon finger

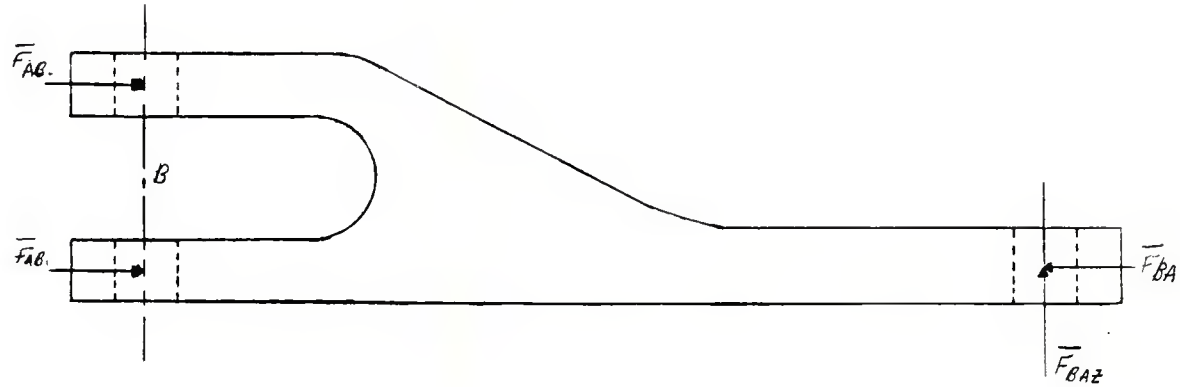


Figure 13. Forces acting upon yoke

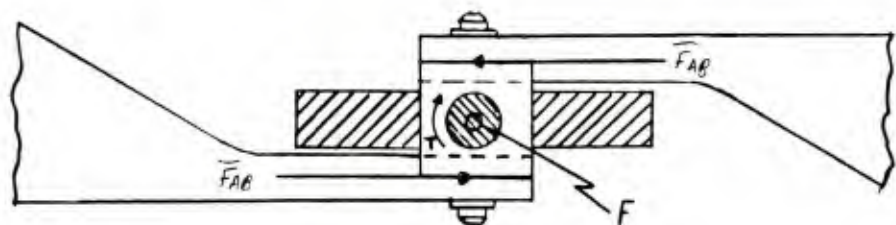


Figure 14. Forces acting upon yoke connector

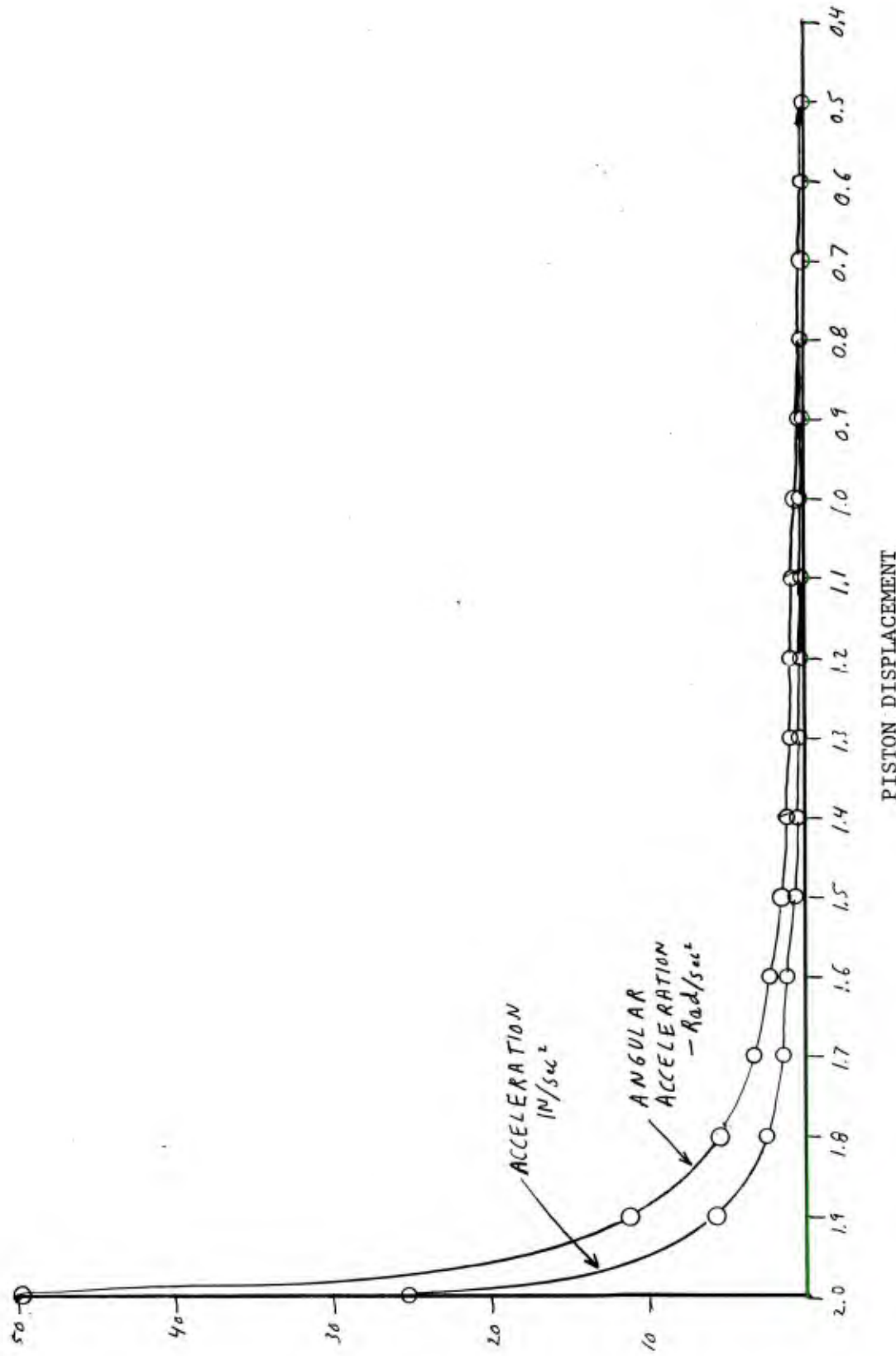


Figure 15. Angular acceleration and acceleration of center of gravity of link 3 versus piston displacement

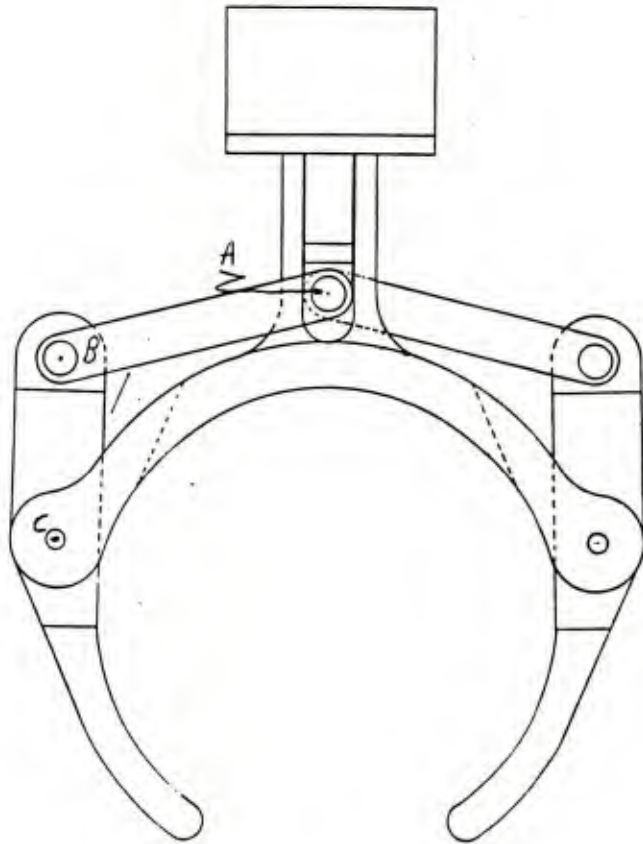


Figure 16. Pin locations

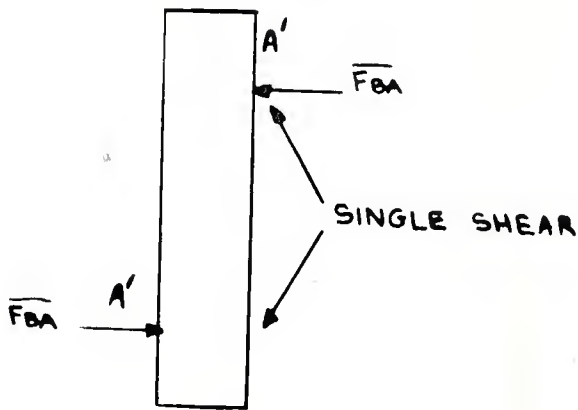


Figure 17. Stress locations on pin at point A

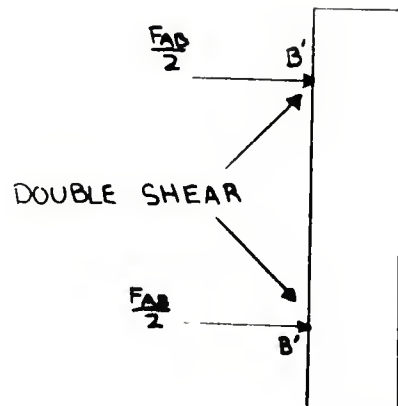


Figure 18. Stress locations on pin at point B

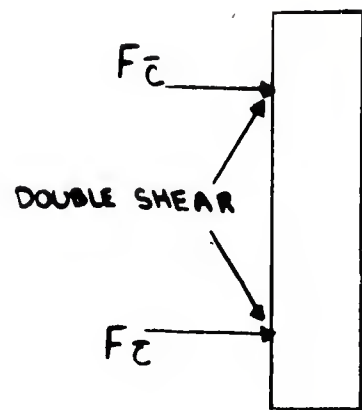


Figure 19. Stress locations on pin at point C

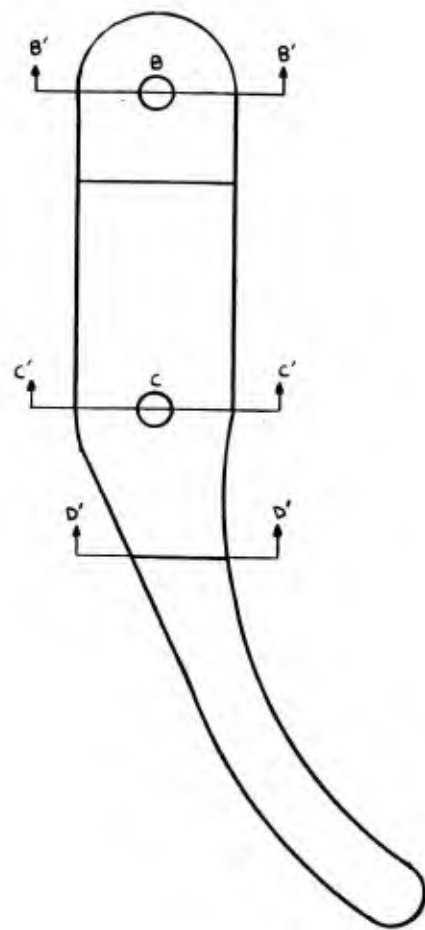


Figure 20. Stress locations on finger

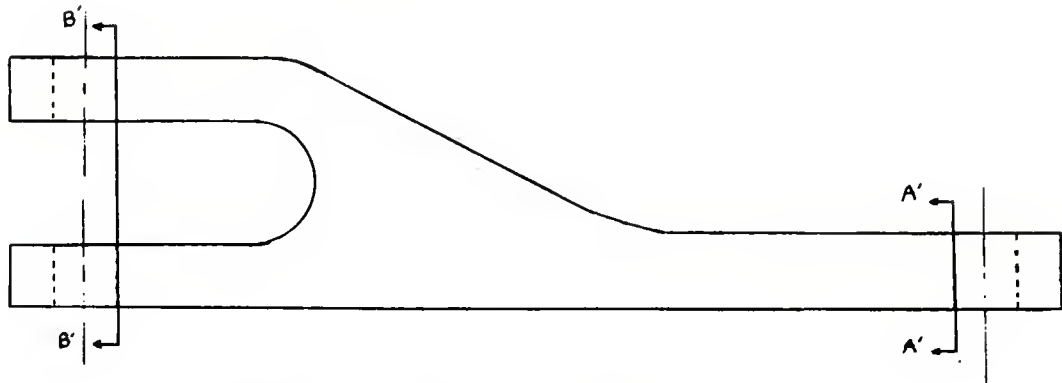


Figure 21. Stress locations on yoke

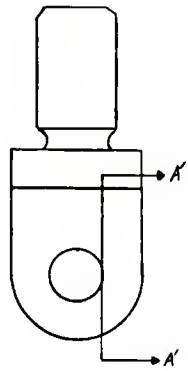


Figure 22. Stress location on yoke connector

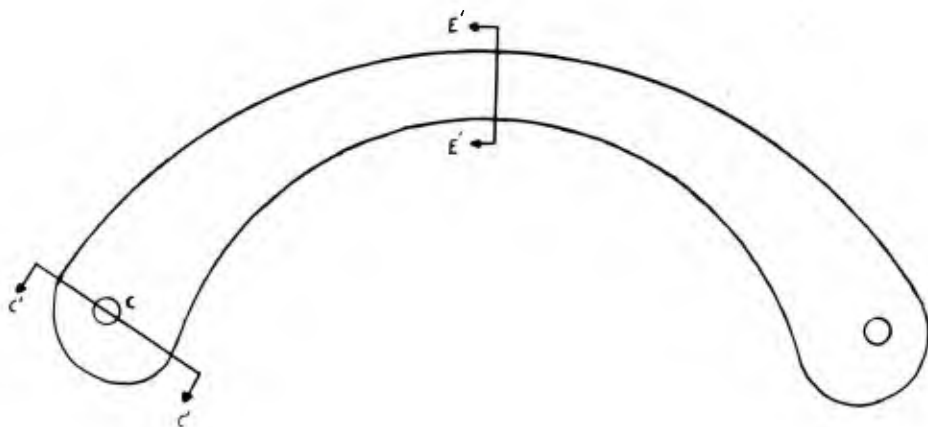
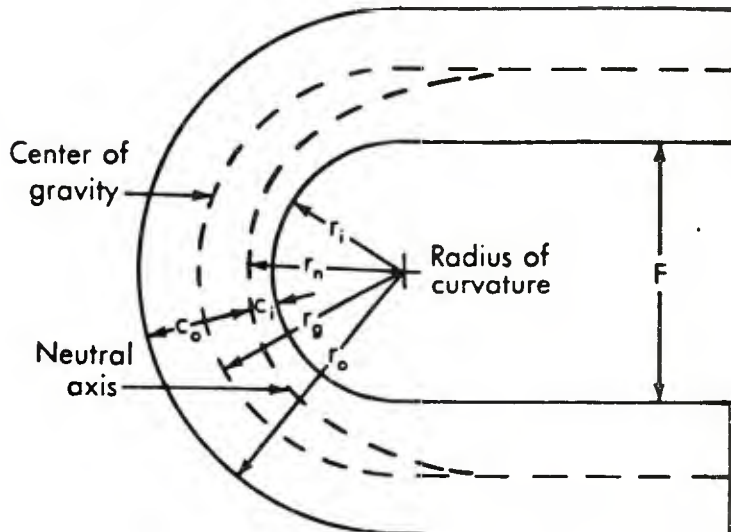


Figure 23. Stress locations on saddle



where:

$A$  = area of cross-section

$e$  = shift of neutral axis from C.G. =  $r_o - r_n$

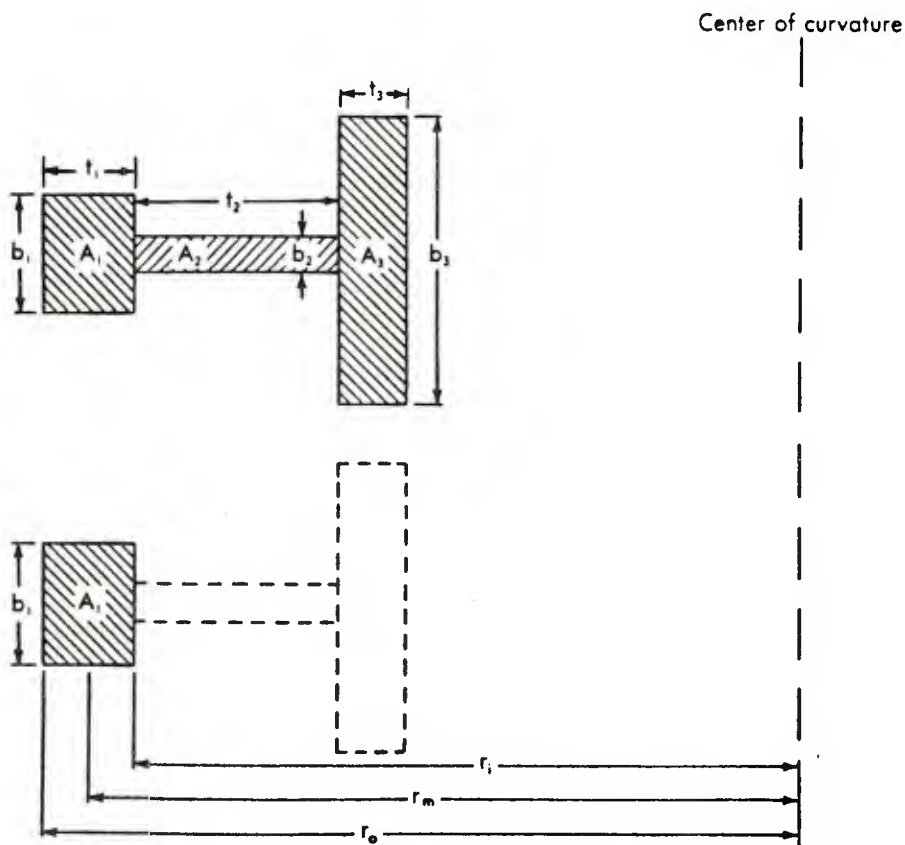
$r_n$  = radius neutral axis from center of curvature

$c_o$  = distance outer fiber to neutral axis =  $r_o - r_n$

$c_i$  = distance inner fiber to neutral axis =  $r_n - r_i$

$r_e$  = radius center of gravity from center of curvature

$d$  = distance line of force to neutral axis of section



Excerpt from Design of Weldments by Omer W. Blodgett, printed by The James F. Lincoln Arc Welding Foundation, Cleveland, Ohio, 1963.

Figure 24. Curved beam analysis

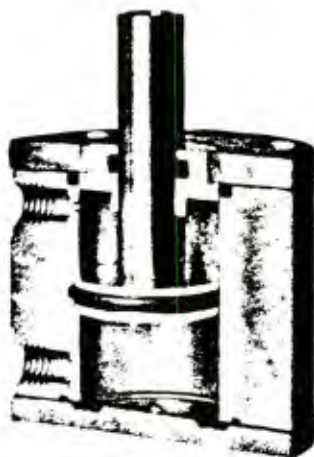


Figure 25. "Pancake" hydraulic cylinder

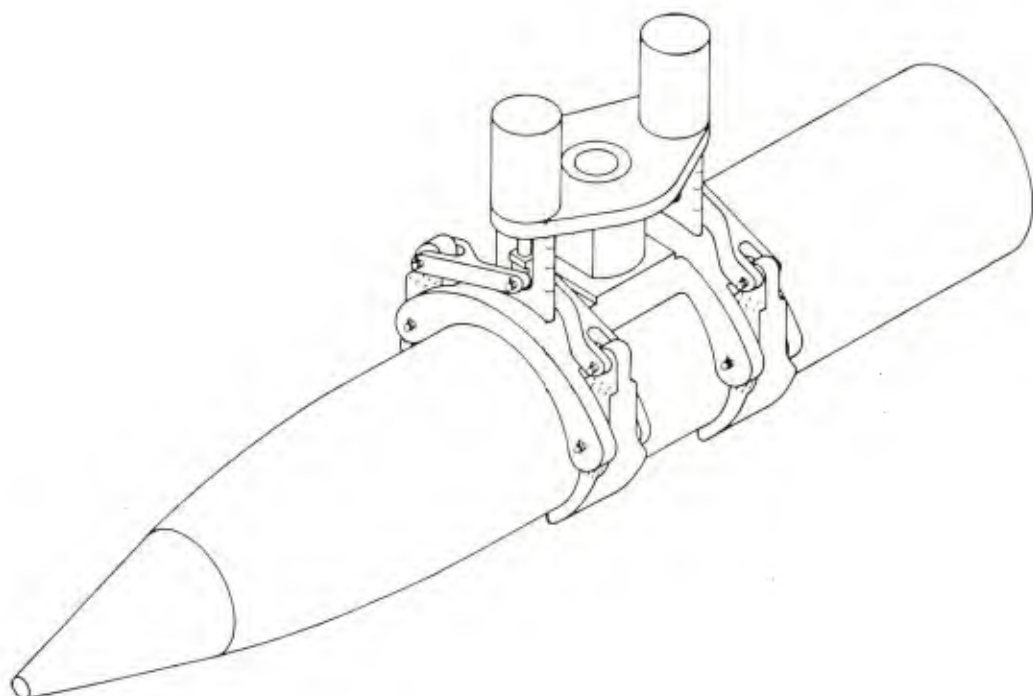


Figure 26. ISAS robotic gripper

APPENDIX A

PRODUCT SEARCH

<u>Manufacturer</u>	<u>Gripper evaluation</u>	<u>Applicability</u>	<u>Remarks</u>
O. S. Walker Co., Inc.	Magnetic force only;	No	
PHD, Inc.	Not enough force; gripper too small.	No	
Mack Corporation			Not interested
VSI Automation	Assembly gripper.	No	
Compact Air Products	Working diameter is less than 6 in., maximum opening is 5 in.; possible to redesign.	Possible	
Simirt	Not enough force (10 lb max).	No	
R&I Mfg. Company, Inc.	Working diameter is less than 6 in. Complete redesign is necessary.	No	
Barrington Automation, Ltd.	Not enough force; gripper too small.	No	
Kennametal, Inc.		No	Primarily metal cutting.
Robohand, Inc.	Not enough force; gripper too small.	No	Willing to design gripper.
Air Technical Industries	Has numerous grippers.	Possible	Needs guidance to choose the best adaptable gripper. Sensors are not included. Customer's design not available. Modificaton probably unavailable. Grippers designed to handle raw material. Grippers usually sold with robots.
Design Technology Corporation		No	Consulting company for automation system.
Positech Corporation		No	Interested only in selling robotic system.
Coleman Equipment, Inc.	Provides variety of grippers.	Perhaps	Needs more specific information.

APPENDIX B  
SPATIAL ANALYSIS  
(DERIVATION OF EQUATIONS, FORTRAN PROGRAM, AND PROGRAM OUTPUT)

## Derivation of Equations

A FORTRAN program was developed to study trends in the mechanism when its characteristics were varied (fig. B-1). Following is the list of variables:

- D Distance between center line of mechanism and low end of piston stroke (in.)
- R Distance between center line of mechanism and lower left hand pin (in.)
- T<sub>2</sub> θ<sub>2</sub> (rad)
- T<sub>1</sub> θ<sub>1</sub> (rad)
- R<sub>2</sub> Length of link R<sub>2</sub> (in.)
- R<sub>3</sub> Length of link R<sub>3</sub> (in.)
- y Longitudinal distance between center line of projectile and lower left-hand pin (in.)
- x Distance gripper displaces (in.)
- S Distance between center pivot and low end of piston stroke (in.)

With the law of cosines, lengths L and h can be determined as a function of R<sub>2</sub>, R<sub>3</sub>, and θ.

$$L^2 = R_2^2 + R_3^2 - 2 R_2 R_3 \cos \theta_2 \quad (B-1)$$

$$h^2 = R_2^2 + R_3^2 - 2 R_2 R_3 \cos \theta_1 \quad (B-2)$$

Subtracting equation B-2 from B-1 yields

$$L^2 - h^2 = - 2 R_2 R_3 \cos \theta_2 + 2 R_2 R_3 \cos \theta_1 \quad (B-3)$$

This equation can be solved for R<sub>2</sub>

$$R_2 = \frac{L^2 - h^2}{2 (\cos \theta_1 - \cos \theta_2) R_3} \quad (B-4)$$

Substituting equation B-4 into B-2 yields

$$L^2 = \left( \frac{L^2 - h^2}{2(\cos \theta_1 - \cos \theta_2)} \right)^2 + R_3^2 - \frac{2R_3(L^2 - h^2) \cos \theta_2}{2R_3(\cos \theta_1 - \cos \theta_2)} \quad (B-5)$$

Multiplying equation B-5 by  $R_3$  and setting it to zero yields

$$R_3^4 - R_3^2 \left( \frac{(L^2 - h^2) \cos \theta_2}{(\cos \theta_1 - \cos \theta_2)} + L^2 \right) + \left( \frac{(L^2 - h^2)}{2(\cos \theta_1 - \cos \theta_2)} \right)^2 = 0 \quad (B-6)$$

Since  $R$  and  $D$  form a right angle, pythagorean theorem can be used to determine  $L$  and  $h$  as a function of  $R$ ,  $D$ , and  $S$

$$L^2 = R^2 + D^2 \quad (B-7)$$

$$h^2 = R^2 + (D + S)^2 \quad (B-8)$$

When equations B-7 and B-8 are substituted into equation B-6 the result is an equation relating  $R_3$  to known parameters

$$R_3^4 - R_3^2 \left( \frac{\left( (R^2 + D^2) - (R^2 + (D + S)^2) \right) \cos \theta_2}{(\cos \theta_1 - \cos \theta_2)} + R^2 + D^2 \right) + \left( \frac{\left( (R^2 + D^2) - (R^2 + (D + S)^2) \right)}{2(\cos \theta_1 - \cos \theta_2)} \right)^2 = 0 \quad (B-9)$$

$$R_3^4 - R_3^2 \left( \frac{\left( D^2 - (D + S)^2 \right) \cos \theta_2}{(\cos \theta_1 - \cos \theta_2)} + R^2 + D^2 \right) + \left( \frac{D^2 - (D + S)^2}{2(\cos \theta_1 - \cos \theta_2)} \right)^2 = 0 \quad (B-10)$$

There are four roots to this equation, two pairs of which are equal. Of the two remaining, one is positive. To find this root the following steps may be used.

Let A and B equal the following:

$$A = - \frac{(D^2 - (D + S)^2) \cos \theta_2}{(\cos \theta_1 - \cos \theta_2)} + R^2 + D^2 \quad (B-11)$$

$$B = \frac{D^2 - (D + S)^2}{2(\cos \theta_1 - \cos \theta_2)} \quad (B-12)$$

$R_3$  can now be found.

$$R_3 = + \left( -\frac{A}{2} \pm \frac{(-A^2 - 4B)^{1/2}}{2} \right)^{1/2} \quad (B-13)$$

Since  $R_3$  is known,  $R_2$  can be determined by equation B-4.

$$R_2 = \frac{L^2 - h^2}{2(\cos \theta_1 - \cos \theta_2) R_3} \quad (B-4)$$

$$R_2 = \frac{D^2 - (D + S)^2}{2(\cos \theta_1 - \cos \theta_2) R_3} \quad (B-14)$$

Calculations are now made to see if the mechanism stays in its intended envelope. If it stays within the envelope, the link lengths of the mechanism are printed out.

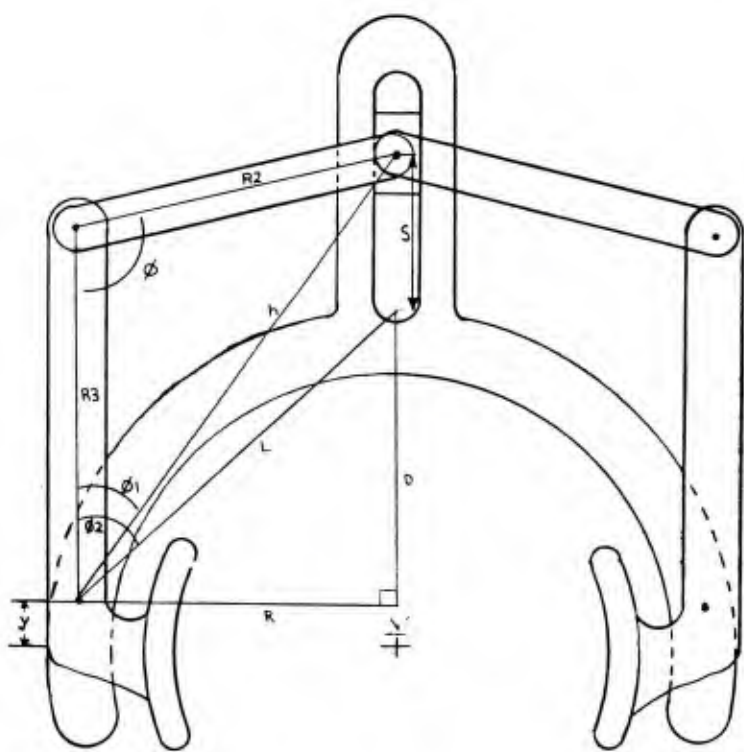


Figure B-1. FORTRAN developed gripper concept

```

PROGRAM MECH 1 (OUTPUT,TAPE6=OUTPUT)
IMPLICIT REAL (A-Z)
COMMON C1
T2=95.*3.1415927/180.
WRITE (6,100)
FORMAT (1H1,12X,'R',9X,'D',9X,'S',8X,'T1',7X,'R3',8X,'R2',9X,'X')
Y=1
C1=0
D050 T1=121,135
T1A=T1*X3.1415927/180.
DO 40 S=.3,1.5,.1
DO 30 R=.3,4.5,.1
DO 20 D=.4,.5,.3,.1
IF (D+S.GT.5.5) GOTO 20
CT=COS(T1A)-COS(T2)
DS=D*D-(D+S)*(D+S)
E=DS*COS(T2)/CT+R*R+D*D
F=(DS/(2*XCT))*X2
IF (E.E.LT.4.*F) GOTO 20
G=(E*X-E-4.*F)**.5
IF (E.LT.G) GOTO 20
R3-((E-G)/2)**.5
CALLHELP (D,R,S,T1A,T2,DS,R3,Y,R2,T1,CT)
R3=R2
CALLHELP (D,R,S,T1A,T2,DS,R3,Y,R2,T1,CT)
CONTINUE
CONTINUE
CONTINUE
STOP
END
SUBROUTINE HELP (D,R,S,T1A,T2,DS,R3,Y,R2,T1,CT)
COMMON C1
R2-DS/2/CT/R3
A=ASIN(R2*SIN(T2)/(R*X*R+D*D)**.5)

```

```

B=ASIN(R2*SIN(T1A)/(R*X*R+(D+S)*(D+S))*X.S)
C=ATAN((D+S)/R)
H=ATAN(D/R)
PH=A-B-C+H
X=Y*SIN(PH)
IF((X.GT..25).AND.(R2*X*COS(3.142-A-T2).LT.4.25)) THEN
  WRITE(6,110) R,D,S,T1,R3,R2,X
  FORMAT(5X,4F10.2,3F10.4)
110
  C1=C1+1
ENDIF
IF(C1.EQ.50) THEN
  WRITE(6,100)
  FORMAT(1H1,12X,'R',9X,'D',9X,'S',8X,'T1',7X,'R3',8X,'R2',9X,'X')
100
  C1=0
ENDIF
RETURN
END

```

Program Output











APPENDIX C

KINEMATIC ANALYSIS

(DERIVATION OF EQUATIONS, FORTRAN PROGRAM, AND SAMPLE PROGRAM OUTPUT)

## Derivation of Equations

The mechanism modeled is shown in figure C-1. Kinematic quantities are determined as a function of piston velocity and displacement. Piston velocity is assumed to be constant. Following is the list of variables used for the analysis.

VA	Velocity of point A (in./sec)
delta	Position of point A from closed position (in.)
W2K	Angular velocity of link R1 in z direction (rad/sec)
W3K	Angular velocity of link R3 in z direction (rad/sec)
Alf2K	Angular acceleration of link R2 in z direction (rad/sec <sup>2</sup> )
Alf3K	Angular acceleration of link R3 in z direction (rad/sec <sup>2</sup> )
T2	Angle theta 2 (deg)
T3	Angle theta 3 (deg)
F	A point on R3
XI	Position of calculated point (x-dir) (in.)
XJ	Position of calculated point (y-dir) (in.)
VI	Velocity of calculated point (x-dir) (in./sec)
VJ	Velocity of calculated point (y-dir) (in./sec)
MAGV	Velocity of calculated point (magnitude) (in./sec)
AI	Acceleration of calculated point (x-dir) (in./sec <sup>2</sup> )
AJ	Acceleration of calculated point (y-dir) (in./sec <sup>2</sup> )
MAGA	Acceleration of calculated point (magnitude) (in./sec <sup>2</sup> )
R	Distance to calculated point from point C (in.)
T	Angle of R from horizontal (rad)

Two approaches can be used to solve  $\theta_2$  and  $\theta_3$ . The law of cosines may be used to relate the geometry in such a way as to produce complex equations which can be solved for  $\theta_2$  and  $\theta_3$ . Since the computer is used for this analysis, a simpler method involving iteration is used. A loop equation can be written to state that the vector sum of all the link lengths is zero. Starting and ending

at the origin and letting  $\hat{i}$  and  $\hat{j}$  be unit vectors in the x and y directions, respectively,

$$- 3.3 \text{ in. } \hat{i} + R_3 (\cos \theta_3 \hat{i} + \sin \theta_3 \hat{j}) + \\ R_2 (\cos \theta_2 \hat{i} + \sin \theta_2 \hat{j}) - ds \hat{j} - 4 \text{ in. } \hat{j} = \bar{0} \quad (C-1)$$

Separating the equation into its  $\hat{i}$  and  $\hat{j}$  components, two scalar equations can be written:

$$- 3.7 \text{ in.} + R_3 \cos \theta_3 + R_2 \cos \theta_2 = 0 \quad (C-2)$$

$$R_3 \sin \theta_3 + R_2 \sin \theta_2 = 0 \quad (C-3)$$

These equations can now be solved for  $\theta_2$  and  $\theta_3$ :

$$\theta_2 = \sin^{-1} ((2.9 \text{ in.} + ds - R_3 \sin \theta_3) / R_2) \quad (C-4)$$

$$\theta_3 = \cos^{-1} ((3.7 \text{ in.} - R_2 \cos \theta_2) / R_3) \quad (C-5)$$

The angular velocities of links  $R_2$  and  $R_3$  can now be determined. The velocity of point A is known, so the velocity of point B can be determined as the velocity of A plus the velocity of point B with respect to point A.

$$\bar{v}_B = \bar{v}_A + \bar{v}_{B/A} \quad (C-6)$$

The velocity of point B with respect to point A is the cross product of the angular velocity of link  $R_2$  ( $\omega_2$ ) with the displacement between points A and B. Assuming  $\omega_2$  is directed in the positive z direction ( $\hat{k}$  unit vector), the following can be written:

$$\bar{v}_{B/A} = \omega_2 \hat{k} \times R_2 (-\cos \theta_2 \hat{i} - \sin \theta_2 \hat{j}) \quad (C-7)$$

Solving the cross product, equation C-6 can be rewritten:

$$\bar{v}_B = v_A \hat{j} - \omega_2 R_2 \cos \theta_2 \hat{j} + \omega_2 R_2 \sin \theta_2 \hat{i} \quad (C-8)$$

In the same manner, it can be written:

$$\bar{v}_B = \bar{v}_C + v_{B/C} \quad (C-9)$$

The velocity of point C is zero,

$$\bar{v}_C = \bar{0} \quad (C-10)$$

The velocity of point B with respect to point C is the cross product of the angular velocity of link  $R_3$  ( $\omega_3$ ) with the displacement between points C and B. As with  $\omega_2$ ,  $\omega_3$  is assumed to be the z direction.

$$\bar{v}_{B/C} = \omega_3 \hat{k} \times R_3 (\cos \theta_3 \hat{i} + \sin \theta_3 \hat{j}) \quad (C-11)$$

Solving the cross product and substituting into equation C-9,

$$\bar{v}_B = \omega_3 \hat{k} \times R_3 (\cos \theta_3 \hat{i} + \sin \theta_3 \hat{j}) \quad (C-12)$$

Equations C-8 and C-12 can be solved and two scalar equations can be written for the x and y directions.

$$v_A - \omega_2 R_2 \cos \theta_2 = \omega_3 R_3 \cos \theta_3 \quad (C-13)$$

$$\omega_2 R_2 \sin \theta_2 = \omega_3 R_3 \sin \theta_3 \quad (C-14)$$

Solving equation C-14 for  $\omega_2$  in terms of  $\omega_3$ ,

$$\omega_2 = -\frac{\omega_3 R_3 \sin \theta_3}{R_2 \sin \theta_2} \quad (C-15)$$

and substituting into equation C-13,

$$v_A + \frac{R_2 R_3 \omega_3 \sin \theta_3 \cos \theta_2}{R_2 \sin \theta_2} = \omega_3 R_3 \cos \theta_3 \quad (C-16)$$

$\omega_3$  can be determined as:

$$\omega_3 = \frac{v_A}{R_3 \cos \theta_3 - \frac{R_3 \cos \theta_2 \sin \theta_3}{\sin \theta_2}} \quad (C-17)$$

Substituting  $\omega_3$  back into equation C-15,  $\omega_2$  can be determined as:

$$\omega_2 = \frac{V_A \sin \theta_3}{R_2 (\sin \theta_2 \cos \theta_3 - \cos \theta_2 \sin \theta_3)} \quad (C-18)$$

The angular acceleration of links  $R_3$  and  $R_3$  is found in the same manner. As with the angular velocities, the angular accelerations are assumed to be in the positive Z direction. The acceleration of point B equals the acceleration of point A plus the acceleration of point B with respect to point A.

$$\bar{a}_B = \bar{a}_A + \bar{a}_{B/A} \quad (C-19)$$

Based on an initial assumption, the acceleration of point A is zero. The acceleration of point B with respect to point A has a normal and tangential component which can be determined by,

$$a_{B/A} = \alpha_2 \hat{k} \times \bar{r}_{B/A} + \omega_2 \hat{k} \times \omega_2 \hat{k} \times \bar{r}_{B/A} \quad (C-20)$$

The vector distance  $\bar{r}_{B/A}$  can be represented in terms of link  $R_2$  and its angle.

$$\bar{r}_{B/A} = R_2 (-\cos \theta_2 \hat{i} - \sin \theta_2 \hat{j}) \quad (C-21)$$

Substituting C-21 into equation C-20 and solving the cross products yields

$$\begin{aligned} \bar{a}_B &= a_{B/A} = -\alpha_2 R_2 \cos \theta_2 \hat{j} + \alpha_2 R_2 \sin \theta_2 \hat{i} + \\ &\quad \omega_2^2 R_2 \cos \theta_2 \hat{i} + \omega_2^2 R_2 \sin \theta_2 \hat{j} \end{aligned} \quad (C-22)$$

The acceleration of point B also equals the sum of the acceleration of point C and the acceleration of point B with respect to point C.

$$\bar{a}_B = \bar{a}_C + \bar{a}_{B/C} \quad (C-23)$$

The acceleration of point C is zero. The acceleration of point B with respect to point C can be solved in the same manner as equation C-19.

$$\bar{a}_B = \alpha_3 \hat{k} \times \bar{r}_{B/C} + \omega_3 \hat{k} \times \omega_3 \hat{k} \times \bar{r}_{B/C} \quad (C-24)$$

The vector distance can be represented in terms of link  $r_3$  and its angle.

$$\bar{r}_{B/C} = R_3 (\cos \theta_3 \hat{i} + \sin \theta_3 \hat{j}) \quad (C-25)$$

Substituting equation C-25 into equation C-24 and solving the cross products yields:

$$\begin{aligned} \bar{a}_B &= \bar{a}_{B/C} = \alpha_3 R_3 \cos \theta_3 \hat{j} - \alpha_3 R_3 \sin \theta_3 \hat{i} - \\ &\quad \omega_3^2 R_3 \cos \theta_3 \hat{i} - \omega_3^2 R_3 \sin \theta_3 \hat{j} \end{aligned} \quad (C-26)$$

By equating C-22 and C-26, an equation can be written for each of the  $\hat{i}$  and  $\hat{j}$  components,

$$\alpha_2 R_2 \sin \theta_2 + \omega_2^2 R_2 \cos \theta_2 = -\alpha_3 R_3 \sin \theta_3 - \omega_3^2 R_3 \cos \theta_3 \quad (C-27)$$

$$-\alpha_2 R_2 \cos \theta_2 + \omega_2^2 R_2 \sin \theta_2 = \alpha_3 R_3 \cos \theta_3 - \omega_3^2 R_3 \sin \theta_3 \quad (C-28)$$

The results are two equations and two unknowns. Solving equation C-27 for  $\alpha_2$  and reducing it yields:

$$\alpha_2 = -\alpha_3 \frac{R_3}{R_2} \frac{\sin \theta_3}{\sin \theta_2} + \omega_3^2 \frac{R_3}{R_2} \frac{\cos \theta_3}{\sin \theta_2} + \omega_2^2 \frac{\cos \theta_2}{\sin \theta_2} \quad (C-29)$$

Equation C-29 can now be substituted into equation C-28 yielding an equation for  $\alpha_3$

$$\begin{aligned} \alpha_3 R_3 \frac{R_2}{R_2} \frac{\cos \theta_2}{\sin \theta_2} \sin \theta_3 + \omega_3^2 R_3 \frac{R_2}{R_2} \frac{\cos \theta_2}{\sin \theta_2} \cos \theta_3 + \omega_2^2 R_2 \frac{\cos^2 \theta_2}{\sin \theta_2} + \\ \omega_2^2 R_2 \sin \theta_2 = \alpha_3 R_3 \cos \theta_3 - \omega_3^2 R_3 \sin \theta_3 \end{aligned} \quad (C-30)$$

$$\begin{aligned} \alpha_3 R_3 \frac{\sin \theta_3}{\tan \theta_2} + \omega_3^2 R_3 \frac{\cos \theta_3}{\tan \theta_2} + \omega_3^2 R_2 \frac{\cos \theta_2}{\tan \theta_2} + \omega_2^2 R_2 \sin \theta_2 = \\ \alpha_3 R_3 \cos \theta_3 - \omega_3^2 R_3 \sin \theta_3 \end{aligned} \quad (C-31)$$

$$\alpha_3 = \frac{\omega_3^2 R_3 \left( \sin \theta_3 + \frac{\cos \theta_3}{\tan \theta_2} \right) + \omega_2^2 R_2 \left( \sin \theta_2 + \frac{\cos \theta_2}{\tan \theta_2} \right)}{R_3 \left( \cos \theta_3 - \frac{\sin \theta_3}{\tan \theta_2} \right)} \quad (C-32)$$

Since  $\alpha_3$  is now known,  $\alpha_2$  can be determined using equation C-29.

$$\alpha_2 = - \left( \alpha_3 \frac{R_3}{R_2} \frac{\sin \theta_3}{\sin \theta_2} + \omega_3^2 \frac{R_3}{R_2} \frac{\cos \theta_3}{\sin \theta_2} + \omega_2^2 \frac{\cos \theta_2}{\sin \theta_2} \right) \quad (C-29)$$

These quantities are used in the computer program to solve for the velocity and acceleration of any given point on the mechanism as a function of piston velocity.

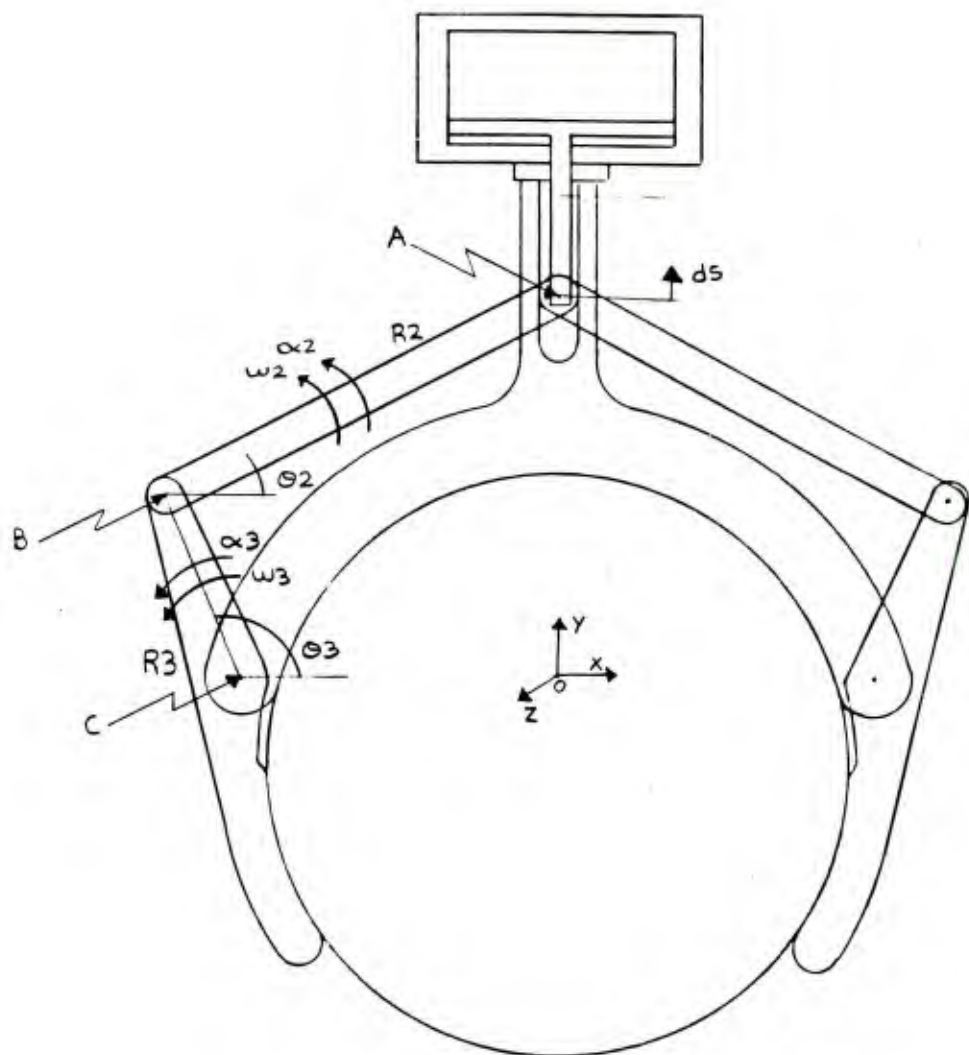


Figure C-1. Kinematic analysis model

```

100= PROGRAM KINEMAT (OUTPUT,TAPE6-OUTPUT)
110= IMPLICIT REAL (A-Z)
120= DIMENSION F(21,10)
130= T3=67.84*X3.1415927/180
140= R2=3.8
150= R3=2.387
160= DO 30 VA=-1,-5,-1
170= WRITE (6,100) VA
180= WRITE (6,110)
190= 100 FORMAT (1H1,10X,"VELOCITY OF A=",F4.1,1X,"INCHES PER SECOND." )
200= 110 FORMAT (6X,"W3K",7X,"ALF3K",8X,"W3K",7X,"ALF3K")
210= DELTS=2.0
220= DO 20 H=1,21
230= DO 10 I=1,500
240= T2=ASIN((2.9+DELTs-R3*SIN(T3))/R2)
250= T3=ACOS((3.7-R2*COS(T2))/R3)
260= 10 CONTINUE
270= ST2=SIN(T2)
280= ST3=SIN(T3)
290= CT2=COS(T2)
300= CT3=COS(T3)
310= W3K=VA/(R3*(CT3-CT2*SIN(T3)/ST2))
320= W2K=-W3K*R3*SIN(T3)/R2/ST2
330= ALF3K=(R3*X3*K*X2*X*(ST3+CT3*SIN(T2)/ST2)+R2*X2*K*X2*X*(ST2+
/CT2/SIN(T2)))/(R3*(CT3-ST3*SIN(T2)/ST2))
340= ALF2K=-(ALF3K*R3/R2*SIN(T3)/ST2+W3K*X2*X*R3/R2*X3*SIN(T2)/ST2)
350= //ST2)
360= R=.5
370= T=T3
380= CALL POINT (R,T,XI,XJ,VI,VJ,MAGU,AI,AJ,MAGA,W3K,ALF3K)
390= F(H,1)=XI
400= F(H,2)=XJ
410= F(H,3)=VI
420= F(H,4)=VJ
430= F(H,5)=MAGU
440= F(H,6)=AI
450= F(H,7)=AJ

```

```

460 F(H,7)=AJ
470 F(H,8)=MAGA
480 T3=T3+(120.-95.)/12.*X3.1415927/180.
490 WRITE(6,240) W2K,ALF2K,W3K,ALF3K
500 FORMAT(1X,4(3X,F8.4))
510 DELTS=DELTs-.1
520 20 CONTINUE
530 WRITE(6,70)
540 70 FORMAT(3(/))
550 200 FORMAT(7X,"XI",10X,"XJ",8X,"VI",10X,"VJ",7X,"MAGU",9X,
560 /"AI",9X,"AJ",8X,"MAGA")
570 210 FORMAT(1X,8(3X,F8.4))
580 WRITE(6,70)
590 WRITE(6,230)
600 230 FORMAT(10X,"POINT F")
610 WRITE(6,200)
620 WRITE(6,210) ((F(I,J),J=1,8),I=1,21)
630 30 CONTINUE
640 STOP
650 END
660 SUBROUTINE POINT(R,T,XI,XJ,VI,VJ,MAGU,AI,AJ,MAGA,W3K,ALF3K)
670 IMPLICIT REAL (A-Z)
680 XI=3.6+RXCOS(T)
690 XJ=RXSIN(T)
700 VI=W3K*RXSIN(T)
710 VJ=W3K*RXCOS(T)
720 MAGU=(VI**2+VJ**2)**.5
730 AI=(ALF3K*XRSIN(T)+W3K*X2*RXCOS(T))
740 AJ=ALF3K*RXCOS(T)-W3K*X2*RXSIN(T)
750 MAGA=(AI*X2+AJ*X2)**.5
760 RETURN
770
780 *EOR
790 *EOF

```

VELOCITY OF A=1.0 INCHES PER SECOND.		ALF3K	U3K
-	2.250	-	-
-	.5994	7.9971	1.2995
-	1.4900	1.8308	.7094
-	4.308	.8830	.5331
-	3.928	.3742	.4359
-	3.659	.2762	.3717
-	3.458	.2131	.3247
-	3.262	.1696	.2880
-	3.076	.1380	.2582
-	3.177	.1140	.2330
-	.2993	.0953	.2111
-	.2923	.0803	.1918
-	.2866	.0679	.1743
-	.2817	.0576	.1583
-	.2776	.0488	.1435
-	.2742	.0412	.1296
-	.2714	.0346	.1164
-	.2681	.0287	.1038
-	.2672	.0235	.0917
-	.2657	.0187	.0683
-	.2646	.0144	.0570

VELOCITY OF A=2.0 INCHES PER SECOND.

	ALF3K	W3K	ALF3K
-1.3519	31.9885	2.4590	-49.9027
-1.1933	37.3231	1.4189	-1.3302
-1.9799	3.5438	1.0662	-15.4965
-1.3617	2.1728	.8719	-3.4054
-1.7656	1.4969	.7433	-2.3875
-1.7318	1.1047	.6494	-1.8052
-1.6916	.8525	.5761	-1.4370
-1.6604	.6785	.5163	-1.1879
-1.6355	.5519	.4659	-1.0111
-1.6152	.4561	.4222	-1.9869
-1.5986	.3812	.3835	-1.7825
-1.5847	.3211	.3486	-1.7066
-1.5731	.2717	.3167	-1.6471
-1.5634	.2304	.2870	-1.6000
-1.5553	.1952	.2592	-1.5625
-1.5485	.1649	.2329	-1.5325
-1.5428	.1383	.2076	-1.5085
-1.5382	.1148	.1833	-1.4894
-1.5344	.0938	.1597	-1.4744
-1.5315	.0749	.1366	-1.4627
			-.4540
			.0576
			.5292

POINT F	XJ	YJ	ZJ	AI	AJ	MAGA
-3.3642	-1.0842	5797	1.2295	20.5777	-14.4315	25.1338
-3.4051	.4605	.2765	.7094	4.8247	-3.1351	5.7538
-3.4336	.4715	.1774	.5331	2.4024	-1.4507	2.8064
-3.4564	.4789	.1252	.4359	1.5218	-1.8530	1.7446
-3.4758	.4843	.3600	.6923	.3717	-1.5642	1.2253
-3.4927	.4883	.3171	.6967	.3247	1.0877	.9269
-3.5076	.4914	.2831	.6532	.2880	.8363	.7374
-3.5214	.4937	.2549	.6408	.2582	.6755	.3997
-3.5332	.4955	.2369	.6311	.2330	.4865	.2958
-3.5442	.4969	.2098	.6236	.2111	.4278	.2254
-3.5542	.4979	.1816	.6176	.1918	.3829	.1754
-3.5633	.4987	.1738	.6128	.1743	.3479	.1691
-3.5716	.4992	.1584	.6090	.1583	.3202	.1665
-3.5792	.4996	.1434	.6060	.1435	.2986	.1637
-3.5860	.4998	.1296	.6036	.1296	.2892	.1615
-3.5921	.4999	.1164	.6018	.1164	.2668	.1613
-3.5976	.5000	.1038	.6005	.1038	.2541	.1628
-3.6025	.5000	.0917	.6005	.0917	.2448	.1656
-3.6068	.5000	.0793	.6011	.0793	.2373	.0995
-3.6105	.4999	.0663	.6014	.0663	.2315	.0945
-3.6136					.2271	.0603

UE

VELOCITY OF A=3.0 INCHES PER SECOND.	
	A LF2X
U2	3.6885
71.9741	**XXXXXX
16.4769	2.1283
-1.4999	-25.4930
1.5993	-12.3672
4.8889	-7.6621
1.2925	-1.3078
-1.1734	1.1150
-1.4397	-5.3718
-1.2374	-4.0616
-1.9996	-3.2332
1.5265	-2.6728
-1.8597	-1.7745
-1.9532	-2.6749
-1.9238	.6989
1.4393	-1.9821
-1.8978	.6333
1.4181	-1.2656
-1.8770	.8577
1.5225	-1.7607
-1.8597	.5753
1.6114	.5229
-1.8451	-1.4561
1.5184	-1.4306
-1.8329	.4393
1.3710	.3888
-1.8227	.3710
1.3112	.3493
-1.8143	-1.1981
1.2583	.3115
-1.8073	-1.1441
-1.8017	.2750
1.2111	-1.1011
-1.7972	.2396
1.1684	-1.0673
-1.7938	.2050
1.1297	-1.0412
	-1.0215

POINT F	XJ	YI	ZK
-3.3642	-1.4409	-1.6264	-1.6264
-3.4051	-1.6095	-1.9800	-1.9800
-3.4336	-1.4789	-1.6264	-1.7540
-3.4564	-1.4843	-1.8883	-1.5400
-3.4758	-1.4914	-1.914	-1.4757
-3.4927	-1.4937	-1.9324	-1.4246
-3.5076	-1.4955	-1.9555	-1.4937
-3.5211	-1.4955	-1.9555	-1.5332
-3.5332	-1.4955	-1.9555	-1.5442
-3.5442	-1.4955	-1.9555	-1.5563
-3.5563	-1.4955	-1.9555	-1.5633
-3.5716	-1.4992	-1.992	-1.5716
-3.5863	-1.4998	-1.998	-1.5863
-3.5921	-1.4999	-1.999	-1.5921
-3.5976	-1.5000	-1.5000	-1.5976
-3.6225	-1.5000	-1.5000	-1.6225
-3.6165	-1.4999	-1.999	-1.6165
-3.6136	-1.4999	-1.999	-1.6136

POINT F	XJ	YI	ZK
UJ	1.8443	1.8696	1.8696
VJ	1.6641	1.4148	1.4148
WJ	1.7996	1.2662	1.2662
XJ	1.6539	1.1878	1.1878
YJ	1.5575	1.1385	1.1385
ZJ	1.4870	1.1045	1.1045
UJ	1.4321	1.0798	1.0798
VJ	1.3824	1.0611	1.0611
WJ	1.3463	1.0467	1.0467
XJ	1.3147	1.0353	1.0353
YJ	1.2864	1.0263	1.0263
ZJ	1.2603	1.0192	1.0192
UJ	1.2371	1.0135	1.0135
VJ	1.2151	1.0090	1.0090
WJ	1.1943	1.0055	1.0055
XJ	1.1746	1.0028	1.0028
YJ	1.1557	1.0007	1.0007
ZJ	1.1375	1.0007	1.0007

POINT F	XJ	YI	ZK
UJ	1.4798	-32.4798	-32.4798
VJ	1.4641	-7.0549	-7.0549
WJ	1.4611	-3.2641	-3.2641
XJ	1.4556	-1.9193	-1.9193
YJ	1.4554	-1.2424	-1.2424
ZJ	1.4473	-2.4473	-2.4473
UJ	1.4415	-1.2694	-1.2694
VJ	1.4254	-2.7569	-2.7569
WJ	1.4254	-2.0855	-2.0855
XJ	1.4193	-1.8993	-1.8993
YJ	1.4193	-1.6656	-1.6656
ZJ	1.4193	-1.5971	-1.5971
UJ	1.4163	-1.3697	-1.3697
VJ	1.4163	-1.3940	-1.3940
WJ	1.4163	-1.3993	-1.3993
XJ	1.4163	-1.4247	-1.4247
YJ	1.4163	-1.4947	-1.4947
ZJ	1.4163	-1.5160	-1.5160



VELOCITY OF A-S.0 INCHES PER SECOND.

	WLF2K	W3K	ALF3K
14.6298	19.9292	6.1476	*****
-12.9959	45.7693	3.5471	-70.8138
-12.4498	22.1486	2.6655	-34.5534
-12.4542	13.5802	2.1797	-21.6837
-11.3640	1.8559	1.8584	-14.9217
-11.8296	6.9944	1.6234	-11.6822
-11.7290	5.3282	1.4402	-8.9812
-11.6509	4.2404	1.2908	-7.4246
-11.5887	3.4494	1.1648	-6.3192
-11.5381	2.8507	1.0555	-5.5058
-11.4964	2.3826	.9588	-4.8908
-11.4617	2.0068	.8716	-4.4163
-11.4328	1.6983	.7917	-4.0446
-11.4085	1.4400	.7176	-3.7503
-11.3882	1.2203	.6481	-3.5157
-11.3712	1.0305	.5822	-3.280
-11.3571	.8645	.5191	-3.1780
-11.3455	.7176	.4583	-3.0587
-11.3361	.5863	.3993	-2.9648
-11.3287	.4679	.3416	-2.8921
-11.3231	.3602	.2849	-2.8375

POINT F	XJ	VI	UJ	AI	AJ	MAGA
XI	4409	1.4494	1.4494	1.4494	1.4494	1.4494
-3.3642	4605	-2.7106	-2.7106	-2.7106	-2.7106	-2.7106
-3.4051	4715	-1.6333	-1.6333	-1.6333	-1.6333	-1.6333
-3.4336	4789	-1.2567	-1.2567	-1.2567	-1.2567	-1.2567
-3.4564	4843	-1.0440	-1.0440	-1.0440	-1.0440	-1.0440
-3.4927	4883	-0.9061	-0.9061	-0.9061	-0.9061	-0.9061
-3.5076	4914	-0.7928	-0.7928	-0.7928	-0.7928	-0.7928
-3.5211	4937	-0.7077	-0.7077	-0.7077	-0.7077	-0.7077
-3.5332	4955	-0.6373	-0.6373	-0.6373	-0.6373	-0.6373
-3.5442	4969	-0.5772	-0.5772	-0.5772	-0.5772	-0.5772
-3.5542	4979	-0.5245	-0.5245	-0.5245	-0.5245	-0.5245
-3.5633	4987	-0.4774	-0.4774	-0.4774	-0.4774	-0.4774
-3.5716	4992	-0.4346	-0.4346	-0.4346	-0.4346	-0.4346
-3.5792	4996	-0.3952	-0.3952	-0.3952	-0.3952	-0.3952
-3.5860	4998	-0.3585	-0.3585	-0.3585	-0.3585	-0.3585
-3.5921	4999	-0.3239	-0.3239	-0.3239	-0.3239	-0.3239
-3.5976	5000	-0.2919	-0.2919	-0.2919	-0.2919	-0.2919
-3.6025	5000	-0.2595	-0.2595	-0.2595	-0.2595	-0.2595
-3.6068	5000	-0.2291	-0.2291	-0.2291	-0.2291	-0.2291
-3.6115	4999	-0.1996	-0.1996	-0.1996	-0.1996	-0.1996
-3.6136	4998	-0.1708	-0.1708	-0.1708	-0.1708	-0.1708

APPENDIX D

DRAWINGS

APPLICATION			REVISIONS																																				
NEXT ASSY	USED ON	SYM	DESCRIPTION	DATE	APPROVAL																																		
83F47C																																							
<p>CYLINDER:</p> <p><math>1\frac{5}{8}</math> BORE - 2 STROKE</p> <p>PART NO. F-221-X</p> <p>SOURCE</p> <p>FABCO - AIR INC. 3716 NE 49TH ROAD GAINESVILLE, FLORIDA 32601</p>																																							
<p>SOURCE CONTROL DWG.</p> <p>PART NO. 83A471</p> <table border="1"> <tr> <td colspan="2">ORIGINAL DATE OF DRAWING 09-30-83</td> <td colspan="4">U S ARMY ARMAMENT RESEARCH AND DEVELOPMENT COMMAND DOVER, NEW JERSEY 07801</td> </tr> <tr> <td>DRAFTSMAN</td> <td>CHECKER</td> <td colspan="4" rowspan="3">CYLINDER, HYDRAULIC</td> </tr> <tr> <td>ENGR</td> <td>ENGR</td> </tr> <tr> <td>ENGR</td> <td>ENGR</td> </tr> <tr> <td colspan="2"></td> <td>SIZE</td> <td>CODE IDENT NO.</td> <td colspan="2">83A471</td> </tr> <tr> <td colspan="2"></td> <td>A</td> <td>19200</td> <td colspan="2"></td> </tr> <tr> <td colspan="2"></td> <td>SCALE</td> <td>UNIT WT</td> <td colspan="2">SHEET</td> </tr> </table>						ORIGINAL DATE OF DRAWING 09-30-83		U S ARMY ARMAMENT RESEARCH AND DEVELOPMENT COMMAND DOVER, NEW JERSEY 07801				DRAFTSMAN	CHECKER	CYLINDER, HYDRAULIC				ENGR	ENGR	ENGR	ENGR			SIZE	CODE IDENT NO.	83A471				A	19200					SCALE	UNIT WT	SHEET	
ORIGINAL DATE OF DRAWING 09-30-83		U S ARMY ARMAMENT RESEARCH AND DEVELOPMENT COMMAND DOVER, NEW JERSEY 07801																																					
DRAFTSMAN	CHECKER	CYLINDER, HYDRAULIC																																					
ENGR	ENGR																																						
ENGR	ENGR																																						
		SIZE	CODE IDENT NO.	83A471																																			
		A	19200																																				
		SCALE	UNIT WT	SHEET																																			

ARRADCOM FORM 65 JUN 78 REPLACES SARPA FORM 1038 OCT 75 WHICH IS OBSOLETE

Figure D-1. Hydraulic cylinder

APPLICATION		REVISIONS			
NEXT ASSY	USED ON	SYM	DESCRIPTION	DATE	APPROVAL
33F470					
SCREW, SOCKET HEAD CAP .190 (NO.10) 32 UNF - 2A X 4 1/2 LG.					
<b>SOURCE</b> FABCO - AIR INC. 3716 NE 99TH ROAD GAINESVILLE, FLORIDA 32601					
<b>SOURCE CONTROL DRAWING</b> <b>PART NO. 83A477</b>					
ORIGINAL DATE OF DRAWING 83-10-27		U S ARMY ARMAMENT RESEARCH AND DEVELOPMENT COMMAND DOVER, NEW JERSEY 07801			
DRAFTSMAN	CHECKER	SCREW, SOCKETHEAD CAP			
ENGR	ENGR				
ENGR	ENGR	SIZE A	CODE IDENT NO. 19200	83A477	

ARRADCOM FORM 65 JUN 78 REPLACES SARPA FORM 1038 OCT 75 WHICH IS OBSOLETE

Figure D-2. Socket head cap screw

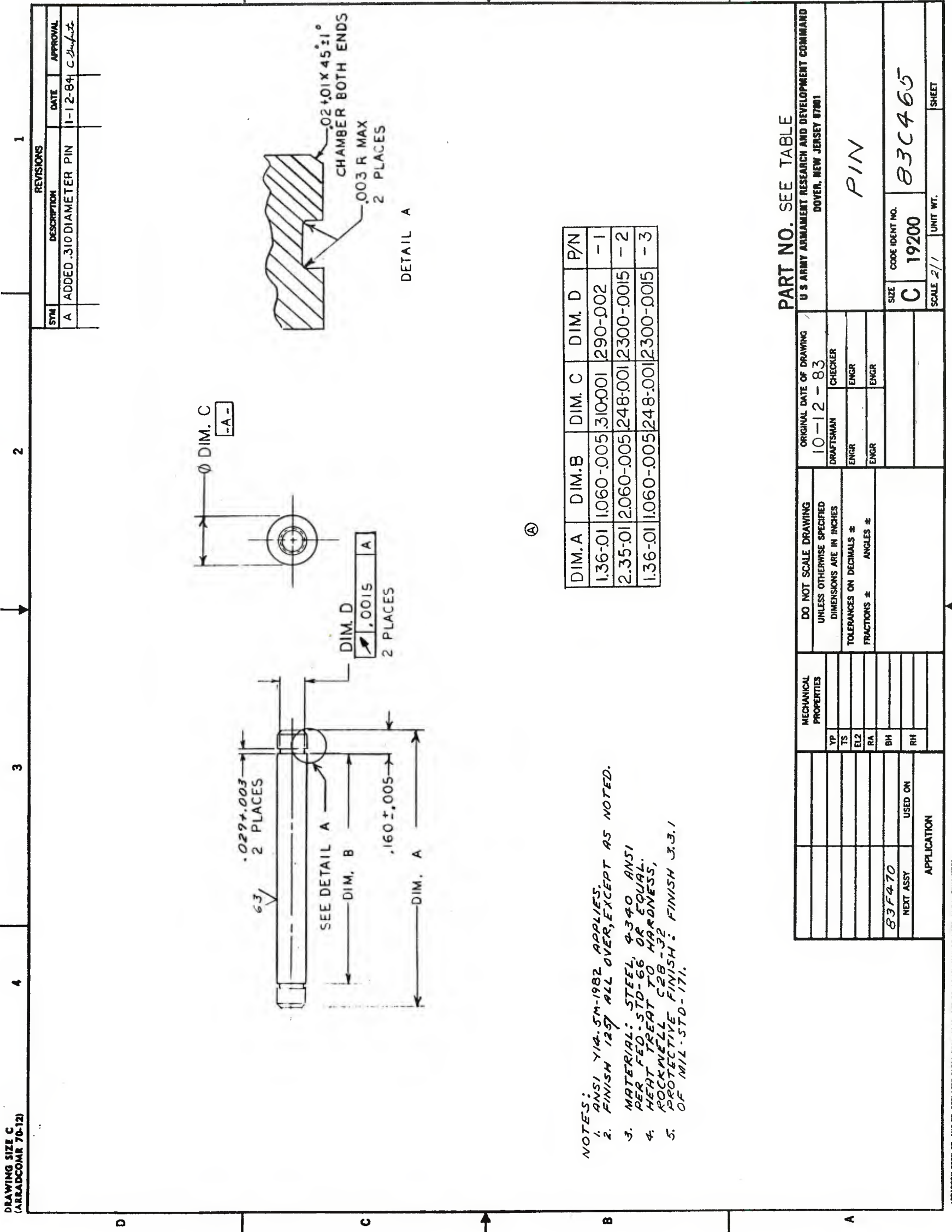


Figure D-3. Pin, part number 83C465

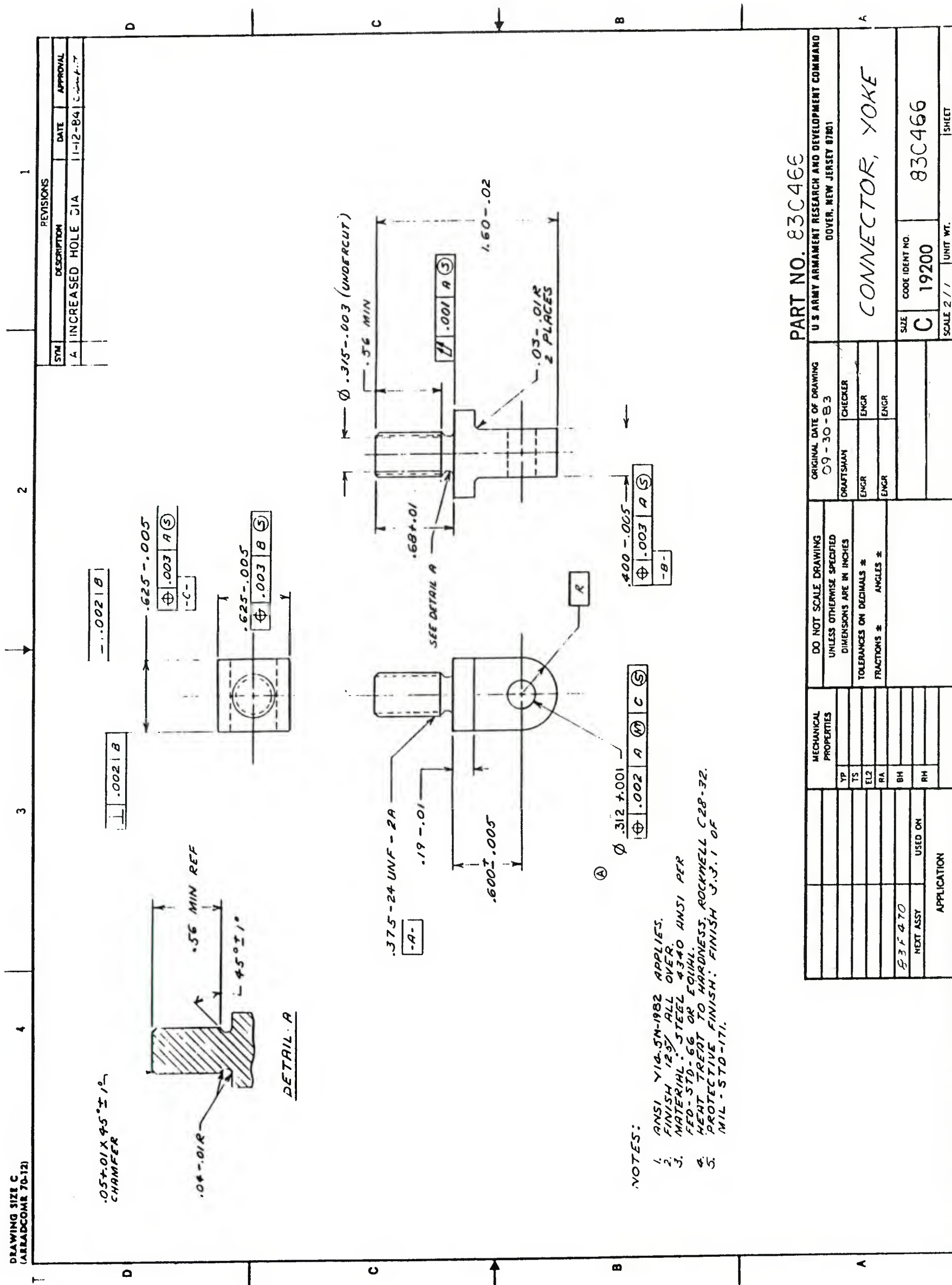
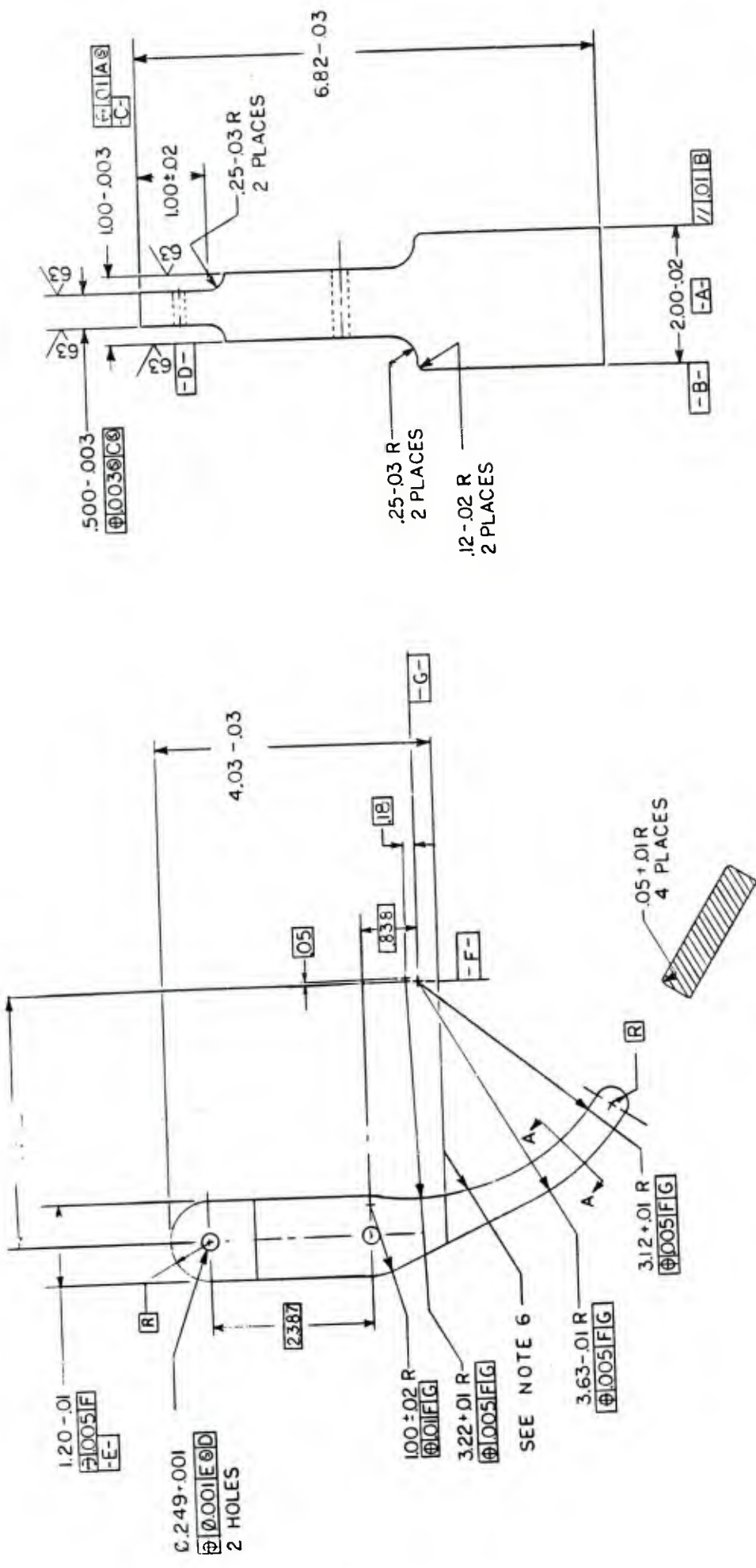


Figure D-4. Yoke connector, part number 83C466



SECTION A-A

- SPEC ANSI Y14.5MH982 APPLIES.
- FINISH  ${}^{+0.01}_{-0.02}$  EXCEPT AS NOTED.
- MATERIAL: STEEL PLATE ALLOY GRADE E, F, G, H, L, M, P, OR Q SPEC ASTM A514.
- HEAT TREAT AND QUENCH TO HARDNESS, RC 28-32.
- PROTECTIVE FINISH: FINISH 3.3.1. OF MIL-STD-171.
- BREAK SHARP CORNER .01 MIN.
- BREAK ALL SHARP CORNERS WITH  $.01 \times .01 \times 45^{\circ} \pm 1^{\circ}$  CHAMFER AND/OR .01 RADIUS.

PART NO. E3E467

U.S. ARMY ARMAMENT RESEARCH AND DEVELOPMENT COMMAND DOVER, NEW JERSEY 07801	
FINGER	
SIZE	CODE IDENT. NO.
D	19200
SCALE 1/1	6.3 D 4 E 7
UNIT WT.	SHEET

Figure D-5. Finger, part number 83D467

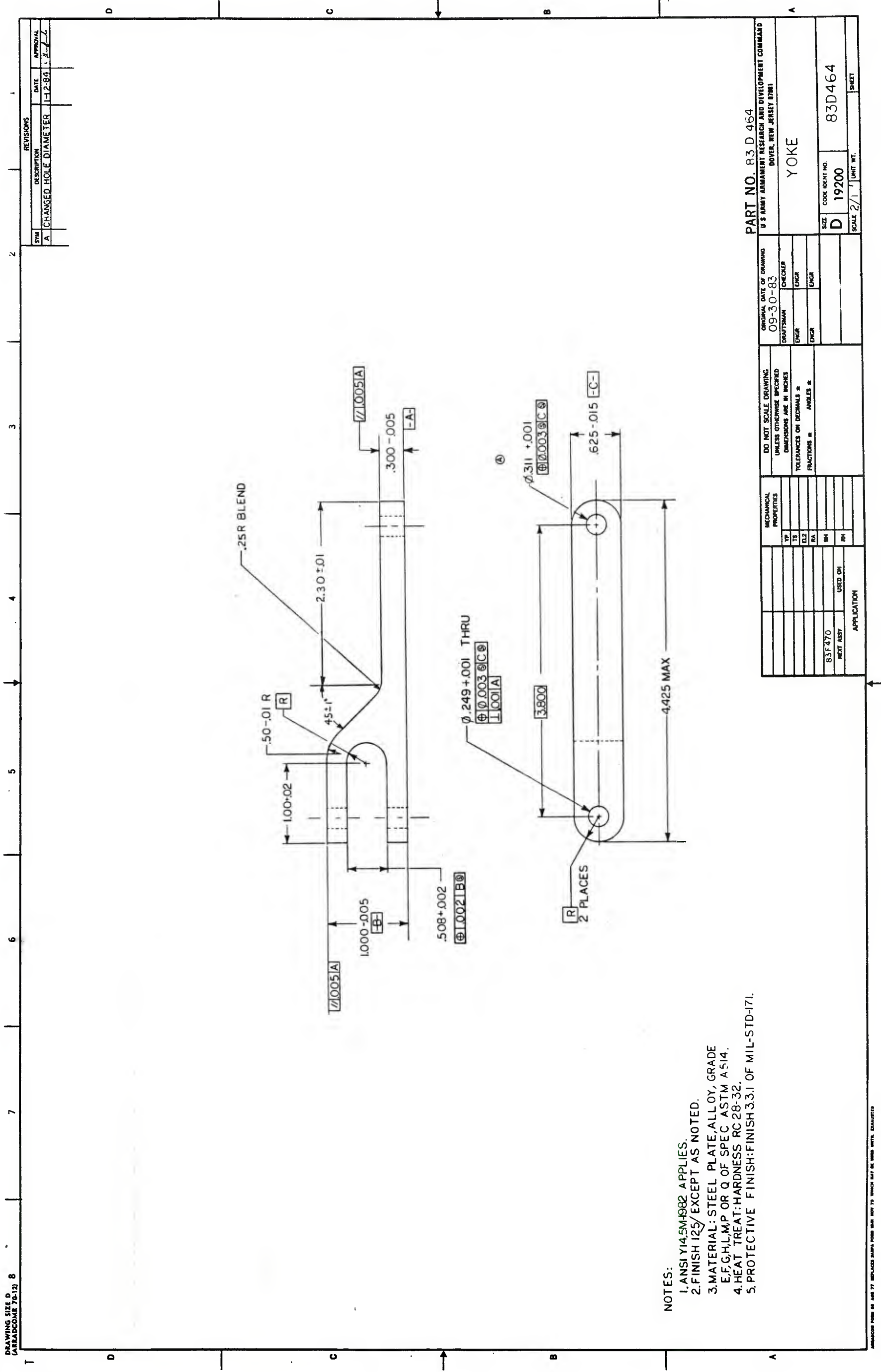


Figure D-6. Yoke, part number 83D464

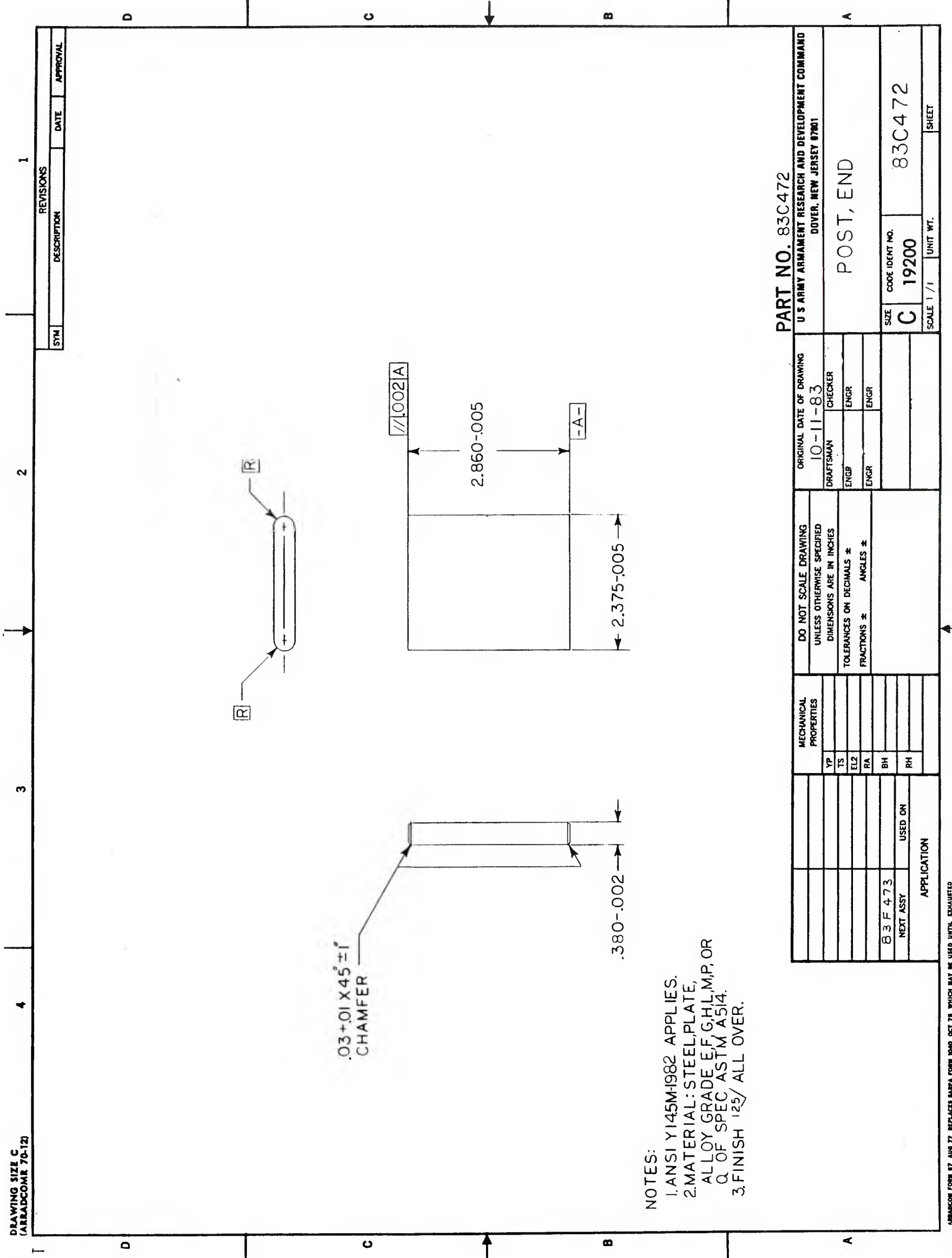


Figure D-7. End post, part number 83C472

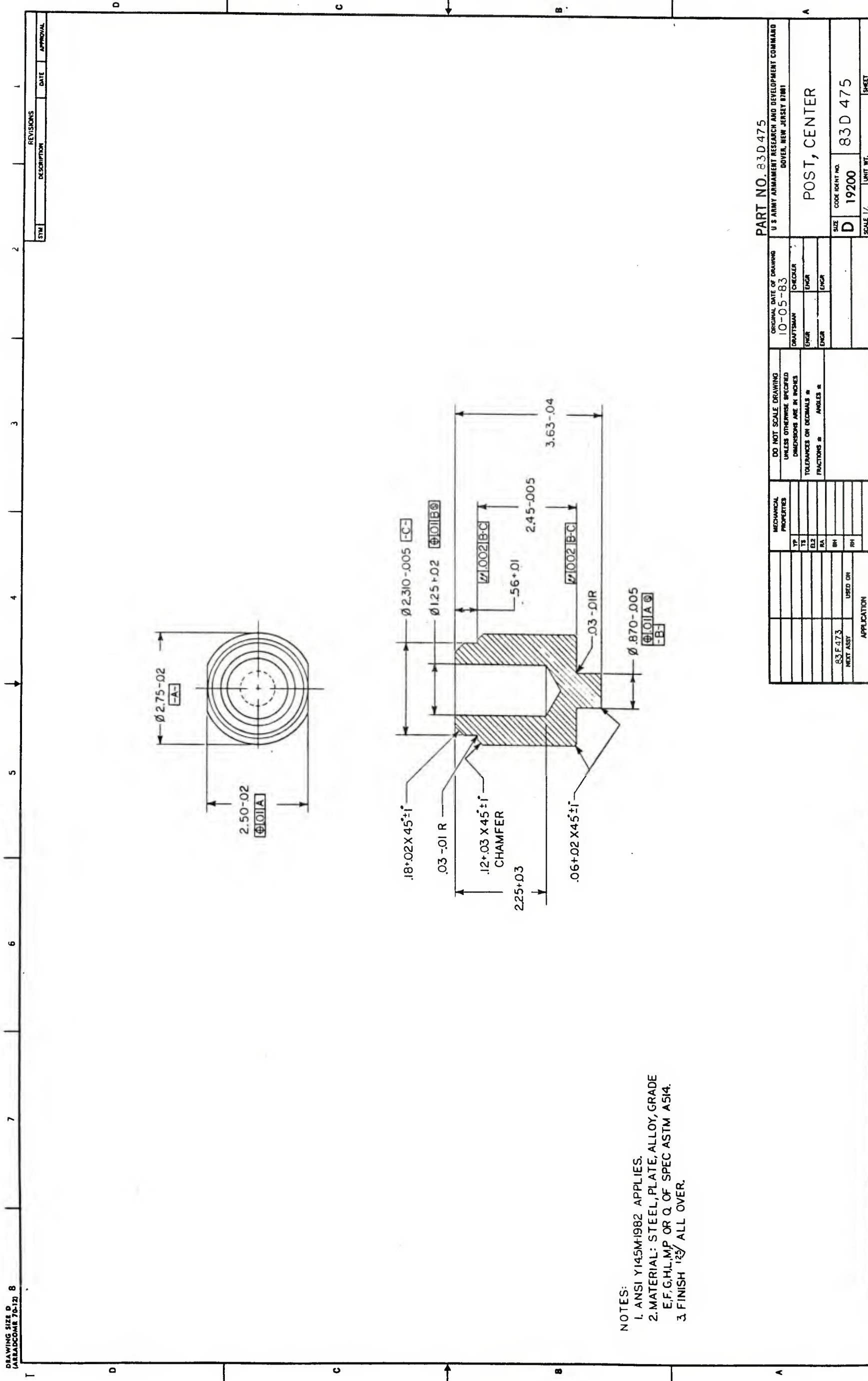


Figure D-8. Center post, part number 83D475

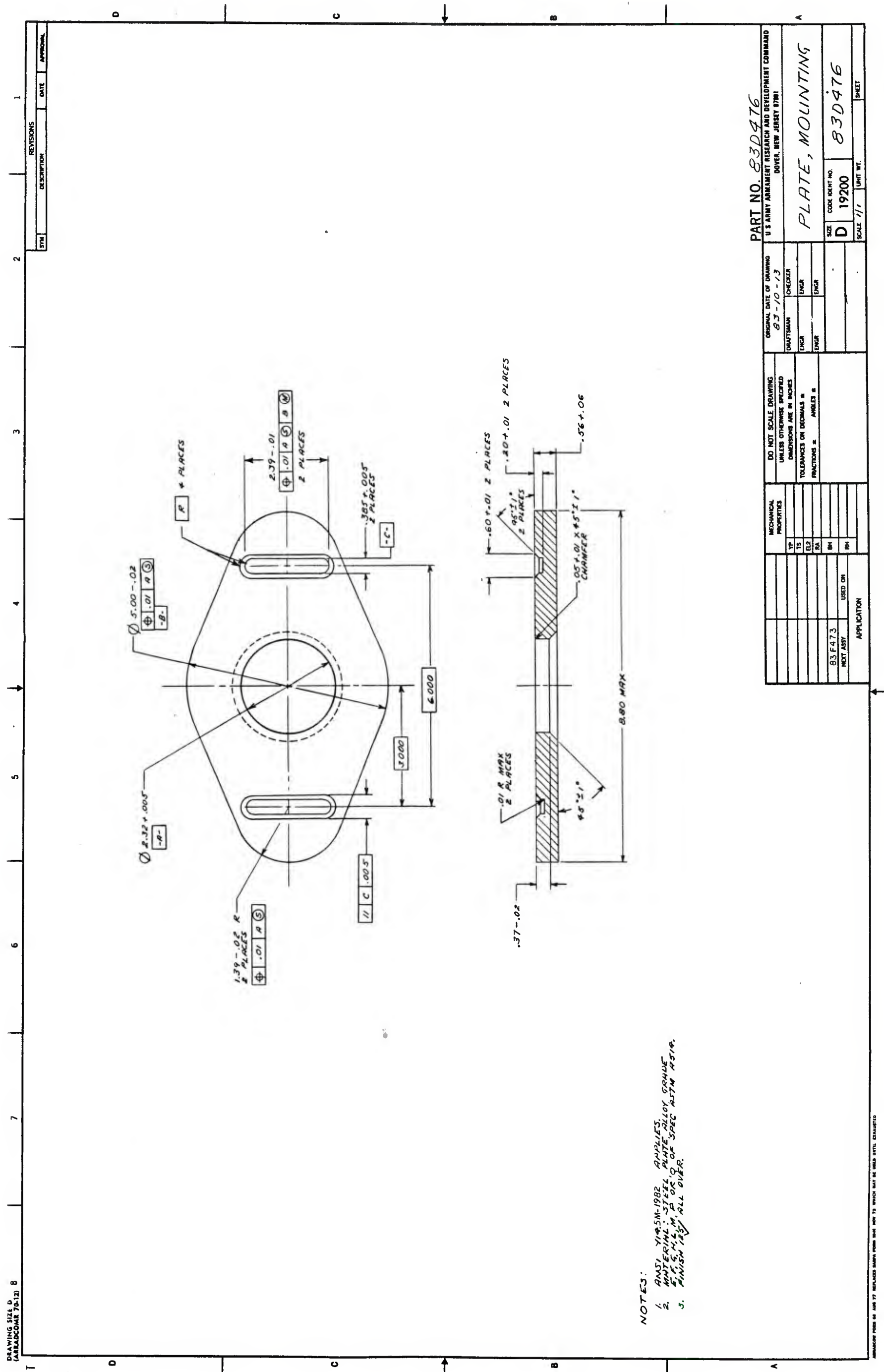


Figure D-9. Mounting Plate, part number 83D476

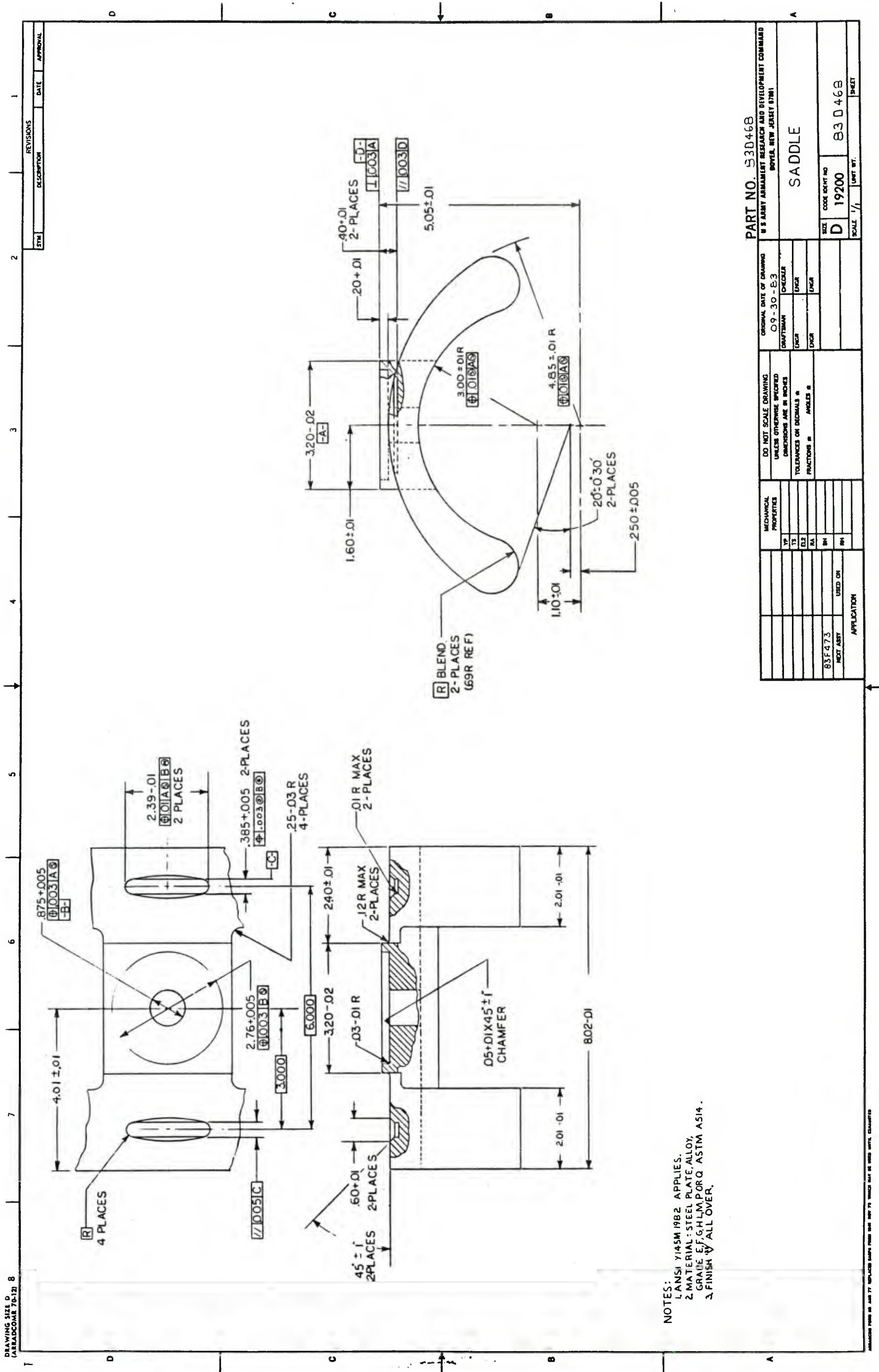


Figure D-10. Saddle, part number 83D468

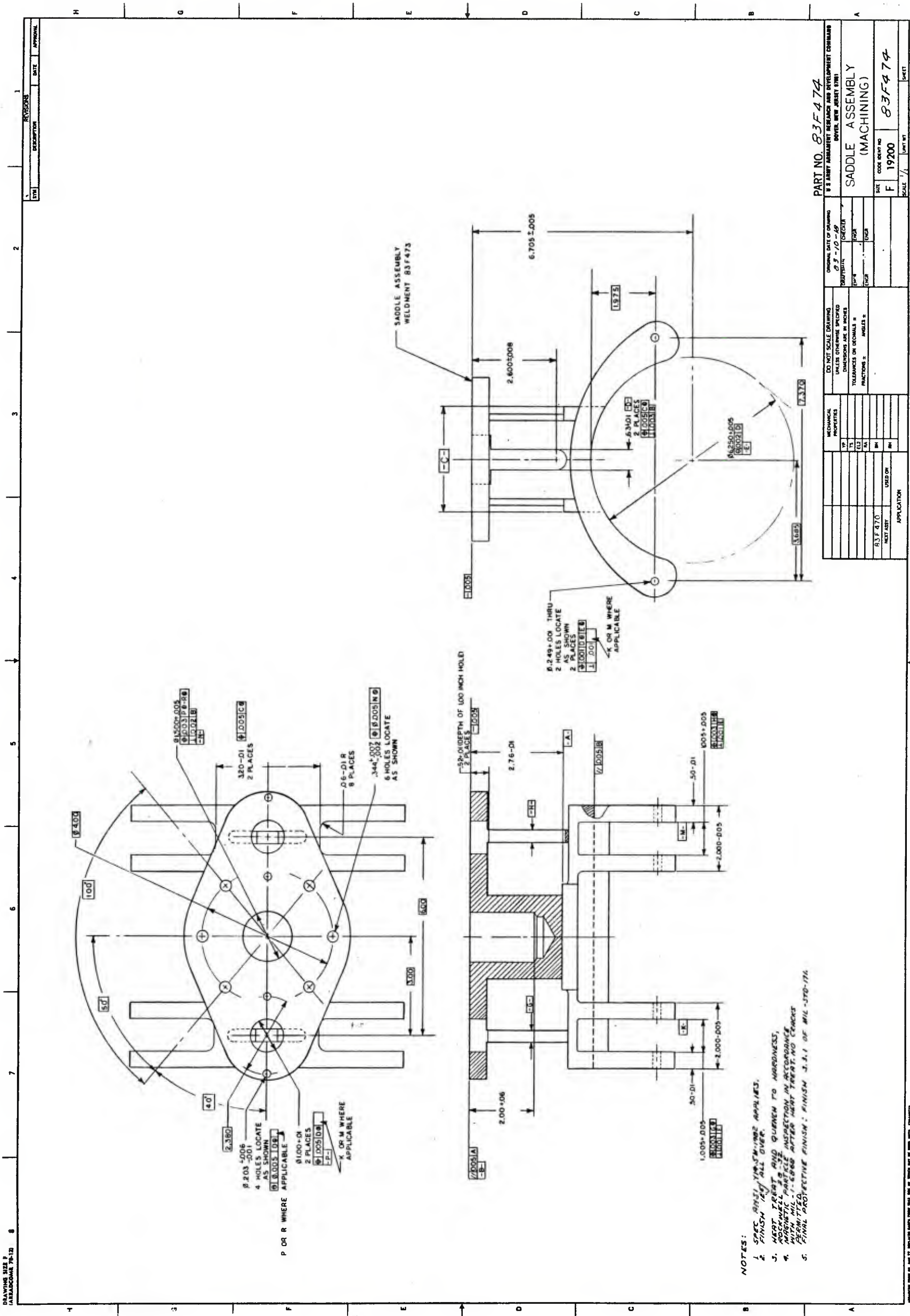
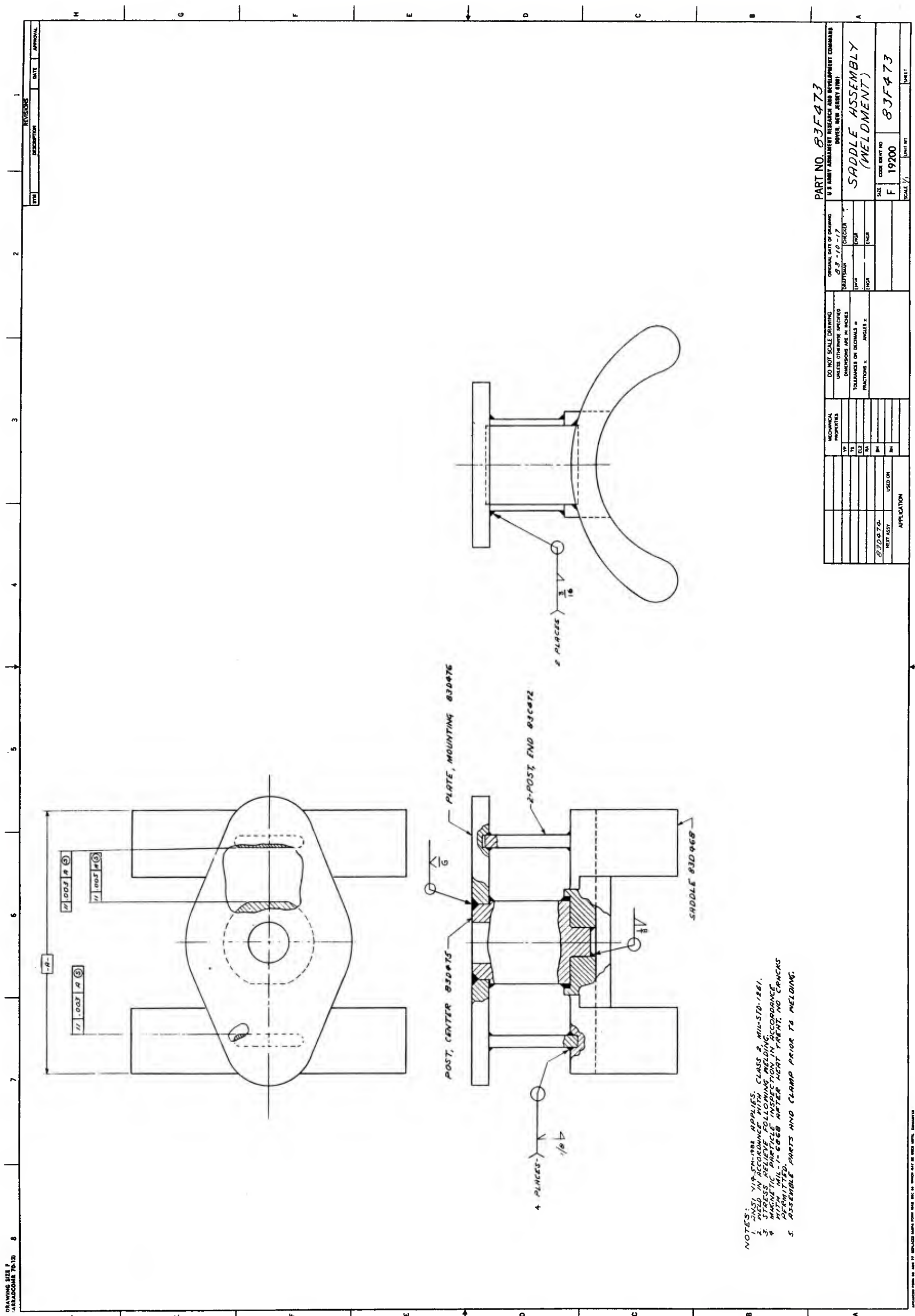


Figure D-11. Saddle assembly (machining), part number 83F474



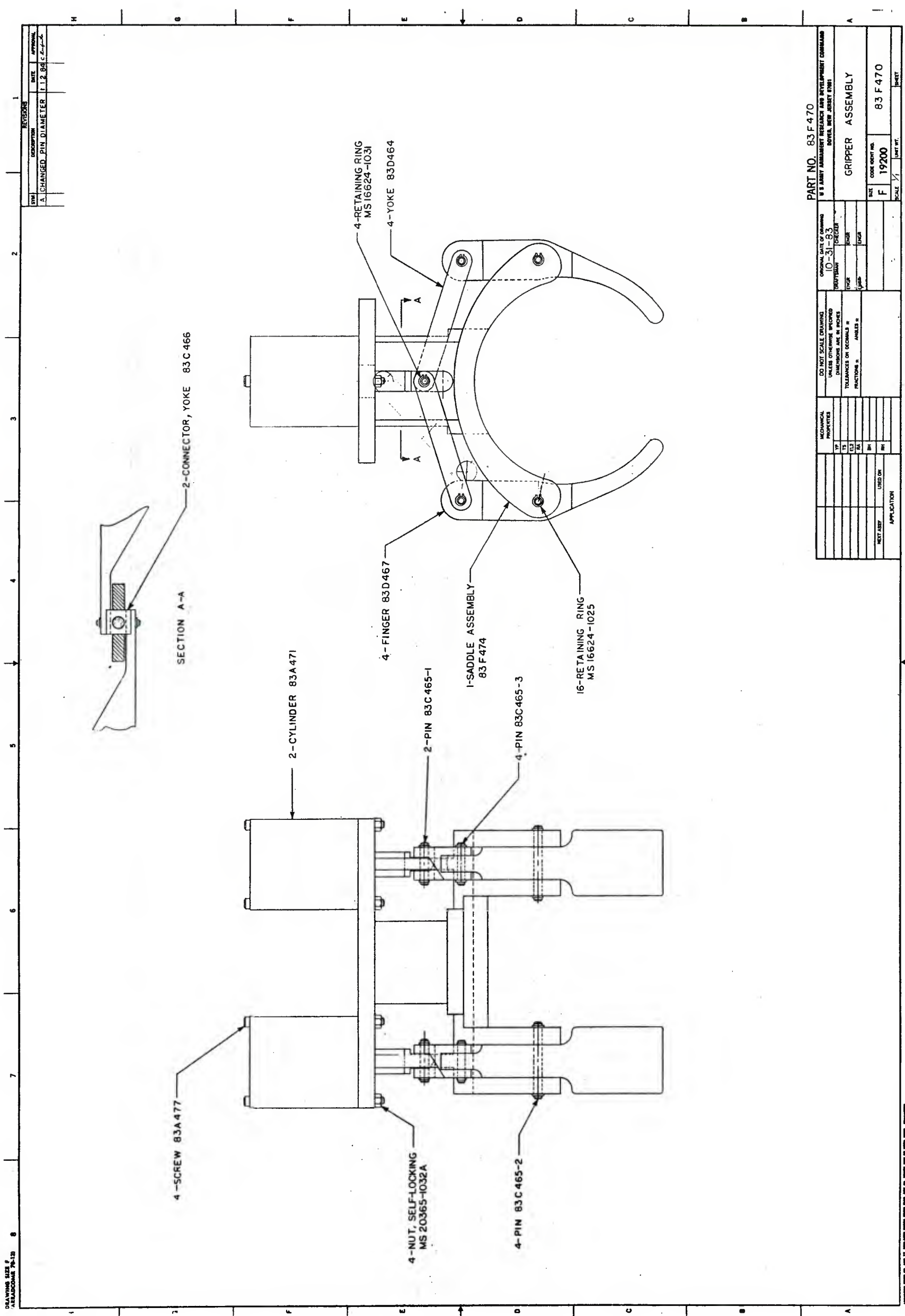


Figure D-13. Gripper assembly, part number 83F470

DISTRIBUTION LIST

Commander  
Armament Research and Development Center  
U.S. Army Armament, Munitions and Chemical Command  
ATTN: SMCAR-TSS (5)  
SMCAR-LC  
SMCAR-LCB  
SMCAR-LCE  
SMCAR-LCM  
SMCAR-LCN  
SMCAR-LCS  
SMCAR-LCU  
SMCAR-LCW (10)  
Dover, NJ 07801-5001

Commander  
U.S. Army Armament, Munitions and Chemical Command  
ATTN: AMSMC-GCL(D)  
Dover, NJ 07801-5001

Administrator  
Defense Technical Information Center  
ATTN: Accessions Division (12)  
Cameron Station  
Alexandria, VA 22314

Director  
U.S. Army Materiel Systems Analysis Activity  
ATTN: DRXSY-MP  
Aberdeen Proving Ground, MD 21005-5066

Commander  
Chemical Research and Development Center  
U.S. Army Armament, Munitions and Chemical Command  
ATTN: SMCCR-SPS-IL  
Aberdeen Proving Ground, MD 21010-5423

Commander  
Chemical Research and Development Center  
U.S. Army Armament, Munitions and Chemical Command  
ATTN: SMCCR-RSP-A  
Aberdeen Proving Ground, MD 21010-5423

Director  
Ballistic Research Laboratory  
ATTN: AMXBR-OD-ST  
Aberdeen Proving Ground, MD 21005-5066

**Chief**

Benet Weapons Laboratory, LCWSL  
Armament Research and Development Center  
U.S. Army Armament, Munitions and Chemical Command  
ATTN: SMCAR-LCB-TL  
Watervliet, NY 12189-5000

**Commander**

U.S. Army Armament, Munitions and Chemical Command  
ATTN: AMSMC-LEP-L  
Rock Island, IL 61299-6000

**Director**

U.S. Army TRADOC Systems Analysis Activity  
ATTN: ATAA-SL  
White Sands Missile Range, NM 88002

Assistant Secretary of the Army  
Research and Development

ATTN: Department for Science and Technology  
The Pentagon  
Washington, DC 20315

**Commander**

U.S. Army Materiel Command  
ATTN: AMC-SG  
5001 Eisenhower Avenue  
Alexandria, VA 22304

**Commander**

U.S. Army Electronics Command  
ATTN: Technical Library  
Ft. Monmouth, NJ 07703

**Commander**

U.S. Army Mobility Equipment Research and Development Command  
ATTN: Technical Library  
Ft. Belvoir, VA 22060

**Commander**

U.S. Army Tank-Automotive Research and Development Command  
ATTN: Tech Library - DRSTA-TSL  
Warren, MI 48090

**Commander**

U.S. Military Academy  
ATTN: CHMN, Mechanical Engineer Dept.  
West Point, NY 10996

**Commander**

U.S. Army Missile Command  
ATTN: Documents Section, Bldg 4484  
Redstone Arsenal, AL 35898

Commander  
Rock Island Arsenal  
ATTN: SMCRI-ENM (Mat Sci Div)  
Rock Island, IL 61299

Commander  
HO, U.S. Army Aviation School  
ATTN: Office of the Librarian  
Ft. Rucker, AL 36362

Commander  
U.S. Army Foreign Science and Technology Center  
ATTN: DRXST-SD  
220 7th Street, N.E.  
Charlottesville, VA 22901

Commander  
U.S. Army Materials and Mechanics Research Center  
ATTN: Technical Library, DRXMR-PL (2)  
Watertown, MA 02172

Commander  
U.S. Army Research Office  
ATTN: Chief IPO  
P.O. Box 12211  
Research Triangle Park, NC 27709

Commander  
Harry Diamond Laboratories  
ATTN: Technical Library  
2800 Powder Mill Road  
Adelphia, MD 20783

Director  
U.S. Naval Research Laboratory  
ATTN: Director, Mech Div  
Code 26-27 (DOC Library)  
Washington, DC 20375

Mechanical Properties Data Center  
Battelle Columbus Laboratory  
505 King Avenue  
Columbus, OH 43201

Commander  
Naval Surface Weapons Center  
ATTN: Technical Library  
Code X212  
Dahlgren, VA 22448